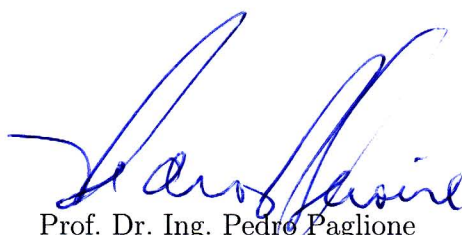


Thesis presented to the Faculty of the Department of Graduate Studies of the Aeronautics Institute of Technology, in partial fulfillment of the requirements for the Degree of Master in Science in the Course of Aeronautical and Mechanical Engineering Flight Mechanics

Gustavo Oliveira Violato

NONLINEAR ADAPTIVE CONTROL SYSTEM FOR PAYLOAD EXTRACTION OPERATIONS.

Thesis approved in its final version by signatories below:



Prof. Dr. Ing. Pedro Paglione

Advisor

Prof. Dr. Celso Massaki Hirata

Head of the Faculty of the Department of Graduate Studies

Campo Montenegro

São José dos Campos, SP - Brazil

2012

Cataloging-in Publication Data

Division of Central Library of ITA/CTA

Oliveira Violato, Gustavo

Nonlinear Adaptive Control System for Payload Extraction Operations. / Gustavo Oliveira Violato.

São José dos Campos, 2012.

86f.

Thesis of Master in Science – Course of Aeronautical and Mechanical Engineering Flight Mechanics – Aeronautical Institute of Technology, 2012. Advisor: Prof. Dr. Ing. Pedro Paglione.

1. Nonlinear control. 2. Flight Mechanics. 3. Aircraft Control. 4. Adaptive Control. I. Aerospace Technical Center. Aeronautics Institute of Technology. Division of Aeronautical Engineering. II. Title.

BIBLIOGRAPHIC REFERENCE

OLIVEIRA VIOLATO, Gustavo. **Nonlinear Adaptive Control System for Payload Extraction Operations..** 2012. 86f. Thesis of Master in Science – Technological Institute of Aeronautics, São José dos Campos.

CESSION OF RIGHTS

AUTHOR NAME: Gustavo Oliveira Violato

PUBLICATION TITLE: Nonlinear Adaptive Control System for Payload Extraction Operations..

TYPE OF PUBLICATION/YEAR: Master Thesis / 2012

It is granted to Aeronautics Institute of Technology permission to reproduce copies of this thesis and to only loan or to sell copies for academic and scientific purposes. The author reserves other publication rights and no part of this thesis can be reproduced without the authorization of the author.

Gustavo Oliveira Violato

Rua Manoel Correia de Freitas, 1300

CEP 82530-070 – Curitiba–PR–Brasil

NONLINEAR ADAPTIVE CONTROL SYSTEM FOR PAYLOAD EXTRACTION OPERATIONS.

Gustavo Oliveira Violato

Thesis Committee Composition:

Prof. Dr.	Luiz Carlos Sandoval Góes	President	-	ITA
Prof. Dr. Ing.	Pedro Paglione	Advisor	-	ITA
Prof Dr.	Fábio Andrade de Almeida	Member	-	ITA
Dr.	Fernando José de Oliveira Moreira	External Member	-	Embraer

Resumo

Este trabalho aborda o problema do desenvolvimento de um sistema de controle não-linear adaptativo para auxiliar a realização de manobras de alijamento de carga. A manobra é crítica pois o deslocamento da carga paga pode tornar a dinâmica do vôo longitudinal instável. A estratégia de controle por meio da adaptação *online* dos parâmetros do controlador parece ser adequada, já que pode lidar com a variação de parâmetros da dinâmica do sistema decorrente da movimentação interna da carga. Os efeitos da variação contínua da posição do C.G. da aeronave na dinâmica de vôo longitudinal são modelados detalhadamente. O controlador proposto consiste na combinação da técnica de inversão dinâmica com a de controle adaptativo por modelo de referência, esta última para lidar com a dinâmica não-modelada ou não conhecida. O sistema dinâmico a ser controlado consiste da dinâmica natural da aeronave aumentada dos parâmetros desconhecidos, cuja dinâmica é controlada pelas leis de adaptação. A demonstração de que as leis de controle e adaptação de parâmetros estabilizam a dinâmica completa é demonstrada via teoria de estabilidade de Lyapunov. A Função Candidata de Lyapunov utilizada para tal é proposta neste mesmo trabalho. Os resultados das simulações são apresentados e discutidos à luz da teoria e de resultados de aplicações de outras arquiteturas de controladores ao mesmo problema.

Abstract

This work covers the development of a nonlinear, adaptive control system for payload extraction operations. Load extractions are a critical type of maneuver which could make the longitudinal flight dynamics unstable. The online adaptation control strategy seems adequate for the problem, since it can deal with the drift in the plant parameters caused by the movement of the load inside the aircraft. The effects of a continuously varying C.G. position on the longitudinal flight dynamics are modeled in detail. The controller proposed consists on applying the technique of nonlinear inversion coupled with a model reference adaptive controller to deal with the unmodeled/unknown dynamics. The dynamic system considered for the control problem consists of the modeled aircraft dynamics augmented by the unknown parameters - whose dynamics are controlled by the chosen adaptation laws. The demonstration of stability for the complete system is done via Lyapunov's stability theorem for nonlinear dynamic systems. A suitable Lyapunov Function Candidate used for such a demonstration is proposed in this work. Simulation results are presented and discussed based on the theory and on comparison with other control methods performance when applied to the same problem.

List of Figures

FIGURE 1.1 – A C-130 performing a Low-Altitude Payload Extraction manouver. (U.S. Air Force).	14
FIGURE 2.1 – Reference frames R and B	21
FIGURE 2.2 – Relationship between vehicle-carried vertical and body axis systems. (From reference (DUKE; ANTONIEWICZ; KRAMBEER, 1988))	26
FIGURE 2.3 – Geometry for finding airplane lift and pitching moment derivatives. (Following (ROSKAM, 2001))	33
FIGURE 3.1 – The feedback linearization controller block diagram scheme.	42
FIGURE 4.1 – The Model Reference Adaptive Controller	55
FIGURE 4.2 – The Self Tunning Adaptive Controller. From (ASTROM; WITTEN- MARK, 2008)	57
FIGURE 5.1 – Schematics for load positions during extraction	59
FIGURE 5.2 – Interior of a Lockheed Martin’s C-5A Galaxy fuselage being loaded. Notice the rails and inclination. (Courtesy of Lockheed Martin).	60
FIGURE 5.3 – Block diagram for a model-reference adaptive controller (MRAC) for pitch control during load extraction.	63
FIGURE 6.1 – Load extraction simulation with fixed commands. Evolution of the states.	71

FIGURE 6.2 – Load extraction simulation with fixed commands. Variation of the parameters in parameter vector A_1	72
FIGURE 6.3 – Load extraction simulation with the adaptive controller (case 1). Evolution of the states.	73
FIGURE 6.4 – Load extraction simulation with the adaptive controller (case 1). Elevator Command.	73
FIGURE 6.5 – Load extraction simulation with the adaptive controller (case 1). Parameter variation and adaptation.	74
FIGURE 6.6 – Load extraction simulation with the adaptive controller (case 2). Evolution of the states.	75
FIGURE 6.7 – Load extraction simulation with the adaptive controller (case 2). Elevator Command.	75
FIGURE 6.8 – Load extraction simulation with the adaptive controller (case 2). Parameter variation and adaptation.	75
FIGURE 6.9 – Block diagram for the controller to be tuned with structured H_∞ approach.	77
FIGURE 6.10 – Load extraction simulation with the robust controller. Evolution of the states.	77
FIGURE 6.11 – Load extraction simulation with the robust controller. Commands.	77
FIGURE A.1 – Top and side view of the C-5A. ((HEFFLEY; WAYNE, 1972))	86

List of Symbols

In order to avoid occupying an unnecessary large ammount of space and taking into account that most of the notation used in this work is standard in aeronautical texts, the symbols are logically grouped. Consider that the description order always follows the symbols order respectively.

$C.G., N.P.$	Center of Gravity and Neutral Point
I_{yy}	Longitudinal moment of inertia with respect to current $C.G.$ location
S, b, \bar{c}	Wing area, wing span and mean aerodynamic chord
X_{ac}, X_N	Longitudinal position of the aerodynamic center and neutral point as measured from the nose of the aircraft.
X_{cg}, X_{cg0}, X_{cgC}	Aircraft's current $C.G.$ location, empty aircraft $C.G.$ location and cargo load $C.G.$ location measured from the nose of the aircraft
$\bar{X}_{cg}, \bar{X}_{ac}, \bar{X}_N$	$C.G.$, aerodynamic center or neutral point longitudinal positions normalized by the mean aerodynamic chord.

σ	Inclination angle of the cargo rail's ramp with respect to the aircraft's longitudinal axis.
m, m_A, m_C	Aircraft's total mass, mass of the empty aircraft, mass of the cargo load
α, β	Angle of attack, angle of sideslip
ϵ	Average angle of downwash at the horizontal tail.
θ, ϕ, ψ	Aircraft's attitude euler angles.
p, q, r	Aircraft's roll, pitch and yaw rates
d_p, d_a, d_r	Elevator, Aileron and Rudder deflection
$C_{L_{\alpha wf}}, C_{L_{\alpha h}}$	Dependence of the respective lift coefficient with angle of attack for the wing fuselage system and for the horizontal tail alone
$C_{\mathcal{L}}, C_{\mathcal{M}}, C_{\mathcal{N}}$	Roll, pitch and yaw moment coefficients
C_L, C_D, C_Y	Lift, drag and side force coefficients
C_{D_0}, k_1, k	Drag polar curve parameters
$C_{L_{<var>}}, C_{Y_{<var>}}$	Lift or side force coefficient linear dependence on a given variable
$C_{\mathcal{L}_{<var>}}, C_{\mathcal{M}_{<var>}}, C_{\mathcal{N}_{<var>}}$	Roll, pitch and yaw moment coefficients linear dependence on a given variable
$C_{L_0}, C_{\mathcal{M}_0}$	Lift and pitch moment coefficients at steady state, zero angle of attack and zero elevator deflection

\hat{q} Adimensionalized pitch rate. Given by $\frac{g\bar{c}}{2V_0}$

Contents

LIST OF FIGURES	vi
1 INTRODUCTION	13
1.1 Load Extraction Manouvers	13
1.2 A brief history of aircraft nonlinear and adaptive controllers	14
1.3 Control Systems for Payload Extraction	16
1.4 Thesis Structure and contributions	16
2 FLIGHT DYNAMICS	19
2.1 Modelling the Aircraft Dynamics	19
2.1.1 Referentials	20
2.1.2 Aerodynamic Forces and Moments	22
2.1.3 Propulsion Forces and Moments	24
2.1.4 Attitude representations and Transformation Matrices	25
2.2 Longitudinal Equations of Motion	28
2.3 Effects of internal mass displacement on aircraft dynamics	31
2.4 Summary	37
3 NONLINEAR CONTROL	39
3.1 Feedback Linearization	39
3.1.1 The SISO Case	40

3.1.1.1	The Normal Form	42
3.1.2	The MIMO Case	45
3.1.3	Summary of the theory	46
3.2	Lyapunov Analysis of Nonlinear Systems	47
3.3	Lyapunov's direct method and Backstepping	50
3.3.1	Extension to non-autonomous systems	51
4	ADAPTIVE CONTROL	53
4.1	Concepts of Adaptive Controllers	53
4.1.1	The MRAC	54
4.1.2	The STC	56
4.1.3	Summary of the theory	58
5	ADAPTIVE CONTROLLER FOR LOAD EXTRACTION	59
5.1	Dynamics of Payload Extraction	59
5.2	Nonlinear-Adaptive Controller Development	62
6	SIMULATION	70
6.1	Description	70
6.2	Results and Discussion	71
7	FINAL COMMENTS	80
7.1	Conclusion	80
7.2	Suggestions for Future Work	81
	BIBLIOGRAPHY	84
	APPENDIX A – AIRCRAFT MODEL	86

1 Introduction

This work dwells with the design of a nonlinear, adaptive control system for the stabilization of the aircraft's longitudinal fast dynamics during payload extraction manouvers. In this section the basic concepts and the problem at stake are covered in some detail.

1.1 Load Extraction Manouvers

Several kind of payload extraction manouvers are performed as tactical delivery methods in places where there is no runway for an aircraft to land or the terrain is not adequate for aircraft operations, when precise location of the delivery is important.

This kind of manouvers can be done with the aid of a LAPES (low altitude payload extraction system) which involves several systems inside the aircraft - as the parachutes for pulling the load, the pallets and rail system inside the fuselage and of course some kind of stability augmentation system to help the pilot accomplish this normally difficult task.

Load extractions are a critical and dangerous manouver, not only they are done in low altitudes and relatively low velocity, but also, as it shall be shown in chapter [6](#), as the load moves inside the aircraft towards its rear, the aircraft's center of gravity (CG)



FIGURE 1.1 – A C-130 performing a Low-Altitude Payload Extraction maneuver. (U.S. Air Force).

gets dislocated severely affecting the aircraft's dynamics, sometimes even unstabilizing it. This maneuver was already extensively studied from the aircraft control point of view during the decade of the 1960 by works like ([RUTAN; STROUP, 1967](#)).

Since one of the promising applications of adaptive control is to be able to maintain a controlled plant following a desired trajectory even in the presence of unpredictable parameter change (as discussed in ([ASTROM; WITTENMARK, 2008](#))), it seems appropriate to study the development of a LAPES with this control technique.

1.2 A brief history of aircraft nonlinear and adaptive controllers

During the past century, linear control theory - both classic and state space - has reached a level of understanding in theory and application high enough to be considered a well developed technology. The last decades have seen the advent and application of robust

linear controllers, which can deal with plant nonlinearities, at least to a certain degree. Hence, a natural question that comes to mind when studying nonlinear techniques is what does the nonlinear controllers can offer to enhance performance, how much improvement can they bring and at what price (both in complexity and monetary costs).

Based mainly in ([SLOTINE; LI, 1991](#)), some reasons for the study of nonlinear control can be pointed. It is noticed that nonlinear controllers can handle a large range of operation, since their design validity is not based on the assumption that the dynamics will remain close to the linearized dynamics. Nonlinear control methods can also deal with hard nonlinearities, such as saturation, dead-zones and hysteresis, to cite a few, which simply rend the mathematical model non-linearizable. Finally there is an improvement of the control system as a whole when one frees oneself of the (sometimes many) simplifying assumptions considered when designing a linear controller.

Powered by the advances in micro-electronics and related technology and by the need of several engineering fields such as spacecraft control, industrial robotics, process engineering and biomedical engineering nonlinear control has attracted an increasing amount of attention for researchers in the field.

The idea behind adaptive controllers, as presented in ([ASTROM; WITTENMARK, 2008](#)), was first studied within the field of aeronautics in the 1950s, when extensive research on experimental aircraft such as the X-15 was done by NASA. Those aircraft were flying higher and faster then any other before and it was soon noticeable how much the flight regime affected the controlability and sometime even the stability of the aircraft.

The stabilished paradigm for aircraft control used today by commercial manufacturers is the gain schedulling approach, which can itself be considered adaptive, since it tunes the gains of the auto-pilot based on the flight condition relative to the flight envelope.

After theoretical contributions on the 1950s and 1960s, the idea of online system identification and gain tuning was further developed during the 1970s. Proofs for stability under restrictive assumptions came in the early 1980s ([ASTROM; WITTENMARK, 2008](#)). More recently, the connection between robust and adaptive controllers, as well as the advance of research on nonlinear theory gave new insights into the robustness of adaptive controllers.

Among the many works done on the subject of aircraft adaptive controllers, one can cite ([HARMANN *et al.*, 1977](#); [STEIN, 1980](#)).

1.3 Control Systems for Payload Extraction

Payload extraction systems seem to have attracted some attention of the reasearch community, particular in China in the past few years. The flight dynamics of an aircraft with a moving load inside the cargo bay are studied in ([YANLI; ZHONGKE; WEI, 2011](#); [SHAOXIU; CHONGSHUN, 2011](#)).

Control techniques specially applied to the case of load extraction system, as is this work, can be seen in ([YIMENG; WEIGUO; BAONING, 2011](#); [CHEN; SHI, 2010](#)). The first of those, specifically, covers the same method applied in this present work with similar results.

1.4 Thesis Structure and contributions

This chapter presents a brief presentation of Load Extraction systems and the underlying control problem involved.

The second chapter presents yet another derivation for the aircrafts longitudinal dynamics. The most common reference systems, as well as a build up of the forces acting on the aircraft are presented before the derivation of the general motion equations. Only then the equations are symplified to represent the aircraft's motion on the vertical plane.

The first contribution of this work is at the end of chapter two, when the equations of longitudinal dynamics are adapted to the case of the varying *C.G.*, as is the case when a load moves inside the aircraft. All the paramenters, inertial and aerodynamic, which are considered to be altered sensibly during the load displacement are accessed and calculated as a function of the *C.G.* displacement from its original location.

The third chapter presents the general theory behind some of the most common nonlinear control techniques, focusing on Feedback Linearization. An overview and major results from Lyapunov's stability theory are also given. The fourth chapter outlines the Adaptive Control theory, focusing on the Model-Reference Adaptive Controller (MRAC) architecture.

The fifth and sixth chapters present the application of the theory and modelling to the problem of developing an adaptive load extraction fast dynamics controller. The controller and adaptation laws are developed in chapter 5.

The other main contributions of this work are inside the nonlinear, adaptive controller development. The combination between the MRAC and nonlinear inversion seems to be of great interest, since its adaptive part is aimed to attack the major caveat in nonlinear inversion, that is, the inevitable degree of ignorance one has over the model of one's dynamic system or its paramenters (YIMENG; WEIGUO; BAONING, 2011). By developing a technique which is able to continously estimate the system paremters while still maintaining global stability, this drawback of the nonlinear inversion technique can

be addressed. For the proof of stability, Lyapunov's second method was chosen where a quadratic Lyapunov Candidate function (following (SINGH; STEINBERG, 1996)) on the states and parameters is proposed for this particular problem.

The simulation results for various cases are found in chapter 6.

The last chapter presents the conclusion and suggestions for future work following what was presented.

2 Flight Dynamics

2.1 Modelling the Aircraft Dynamics

The dynamics of a rigid aircraft - that is, the dynamics obtained by neglecting the forces caused structural deformations of the aeroplane - is well described by a set of ordinary differential equations on the state variables. Those are obtained from applying the Newton's law of motion for the translational and rotational components of the state.

Following (ETKIN, 1972; DUKE; ANTONIEWICZ; KRAMBEER, 1988; TENENBAUM, 2003), the equations of motion of a body subject to a sum of forces and moments, written in a galilean referential (O) are:

$$\sum \mathbf{F} = \frac{d}{dt} (m {}^O \mathbf{v}^{C^*}) \quad (2.1a)$$

$$\sum \mathbf{M} = \frac{d}{dt} (\mathbb{I}^{O/C^*} \boldsymbol{\Omega}^B) \quad (2.1b)$$

where C^* refers to the center of gravity of the aircraft and (B) is a reference frame centered at the same origin as (O) but rotating together with the aeroplane. Written in

(^B) equations 2.1 become:

$$\mathbf{F}^{\mathcal{F}_a} + \mathbf{F}^{\mathcal{F}_p} + \mathbf{F}^{\mathcal{F}_g} = \frac{d}{dt}(m\mathbf{v}) + \boldsymbol{\Omega} \times (m\mathbf{v}) \quad (2.2a)$$

$$\mathbf{M}^{\mathcal{F}_a} + \mathbf{M}^{\mathcal{F}_p} = \frac{d}{dt}(\mathbb{I}\boldsymbol{\Omega}) + \boldsymbol{\Omega} \times (\mathbb{I}\boldsymbol{\Omega}) \quad (2.2b)$$

Where:

\mathcal{F}_g stands for the *Weight*.

\mathcal{F}_p stands for *Propulsion* forces.

\mathcal{F}_a stands for *Aerodynamic* forces.

And:

$$\mathbb{I} = \begin{bmatrix} I_{xx} & -I_{xy} & -I_{xz} \\ -I_{xy} & I_{yy} & -I_{yz} \\ -I_{xz} & -I_{yz} & I_{zz} \end{bmatrix} \text{ is the inertia matrix of the aircraft.}$$

The challenge of correctly modelling the aircraft dynamics is therefore to determine the forces and moments components generated by the aerodynamic and propulsion external forces.

Normally the equations 2.2 are further simplified by the assumption of constant mass and inertia. In the case of payload extraction, as studied in this work, that is not applicable. The equations for the longitudinal motion of the aircraft with varying inertia are derived in section 2.2

2.1.1 Referentials

The vectors in the equations of motion for the aircraft can be written in any referential. As we will see just below, depending on the nature of the vector (i.e. aerodynamic resultant force or body angular velocity) it becomes more suitable to write it in a particular reference

frame. This is why different vector bases are defined for the description of a plane in flight.

The most used ones are defined below:

The inertial reference frame \mathbf{O} : Considering the “flat earth” referential as an inertial frame (STEVENS; LEWIS, 2003), we can define the *inertial reference* base (see figure 2.1) $\mathbf{O} = \{\mathbf{x}_0, \mathbf{y}_0, \mathbf{z}_0\}$ with \mathbf{x}_0 and \mathbf{y}_0 defining the horizontal plane, \mathbf{x}_0 pointing a given direction (i.e. local north), \mathbf{z}_0 pointing downwards and finally \mathbf{y}_0 in such a way that \mathbf{O} is right-hand positive. This is also called the topodetic reference system as in (DUKE; ANTONIEWICZ; KRAMBEER, 1988).

The body reference frame \mathbf{B} : As the name suggests, the *body reference* base $\mathbf{B} = \{\mathbf{x}_B, \mathbf{y}_B, \mathbf{z}_B\}$ (see figure 2.1) is aligned with the aircraft geometry, being \mathbf{x}_B the aircraft central axis, \mathbf{y}_B pointing to the right wing and \mathbf{z}_B rendering \mathbf{B} a right-hand positive base.

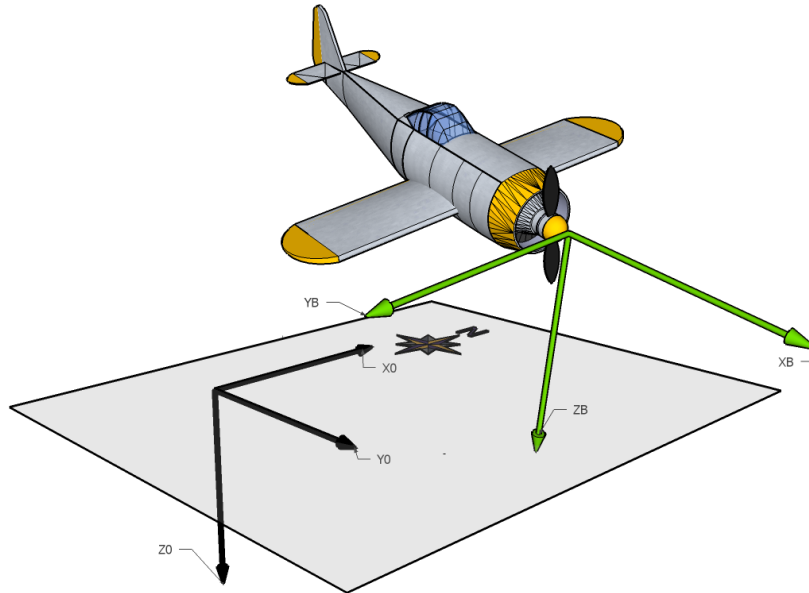


FIGURE 2.1 – Reference frames \mathbf{R} and \mathbf{B}

The wind reference frame \mathbf{W} : This is the frame aligned with the true airspeed velocity vector. The *wind reference* base $\mathbf{W} = \{\mathbf{x}_\mathbf{W}, \mathbf{y}_\mathbf{W}, \mathbf{z}_\mathbf{W}\}$ is defined with $\mathbf{x}_\mathbf{W}$ in the same direction as the true airspeed, pointing away from the aircraft. The other axis are defined in such a way that, when rotated an angle $-\beta$ around the $\mathbf{z}_\mathbf{W}$ axis, and then an angle α around the $\mathbf{y}_\mathbf{W}$ axis, the resulting frame coincides with body frame \mathbf{B} .

The propulsion reference frame \mathbf{P} : Following the same thinking as for the wind reference frame, we define the *propulsion reference* frame $\mathbf{P} = \{\mathbf{x}_\mathbf{P}, \mathbf{y}_\mathbf{P}, \mathbf{z}_\mathbf{P}\}$, as being aligned with the resultant propulsion force vector acting on the aircraft in a given moment. Hence, to transform \mathbf{P} into \mathbf{B} , the rotations are analogous to the described above for the frame \mathbf{W} , but now the angles are α_f and $-\beta_f$

2.1.2 Aerodynamic Forces and Moments

The aerodynamic forces and moments are modelled as in (ETKIN, 1972; NELSON; SMITH, 1989; STEVENS; LEWIS, 2003). The practical objective of the study of aircraft aerodynamics is to give the resultant force and moment acting on the center of gravity of the aircraft for all the expected flight conditions (SCHLICHTING; TRUCKENBRODT, 1979).

The resultant of this force decomposed on the wind reference frame is given by:

$$\mathcal{F}_a = [-D, Y, -L]^T \quad (2.3)$$

The total aerodynamic moment decomposed in the body frame is given by:

$$\mathcal{M}^{\mathcal{F}_a} = [\mathcal{L}, \mathcal{M}, \mathcal{N}]^T \quad (2.4)$$

The study of aerodynamics ([SCHLICHTING; TRUCKENBRODT, 1979](#)) demonstrates that under certain conditions the aerodynamic forces and moments ($\mathcal{F}_a, \mathcal{M}^{\mathcal{F}_a}$) and the flight variables (i.e the angles α and β , the angular velocity components and the control surface deflections) hold a linear relation to each other. The conditions just cited above are that α and β remain relatively small and that the angular velocity rates also remain bounded to certain values. The only exception of this rules being the drag force (D), which approximately holds a parabolic relation with the lift force.

Also, it is common practice in aerodynamics to make all forces and moments adimensionalized, so that these relations described above are given in terms of the aerodynamic coefficients.¹ The reader is asked to refer to ([SCHLICHTING; TRUCKENBRODT, 1979](#)) or ([ROSKAM, 2001](#)) for a complete treatment of the subject. The important result of the above discussion is that it is possible to write each of the aerodynamic coefficients as showed below:

$$C_L = C_{L_0} + C_{L_\alpha} \alpha + \boxed{C_{L_{\bar{q}}}} \frac{q\bar{c}}{2V_{ref}} + C_{L_{d_p}} d_p \quad (2.5a)$$

$$C_Y = C_{Y_\beta} \beta + C_{Y_{\bar{r}}} \frac{rb}{2V_{ref}} + C_{Y_{d_r}} d_r + C_{Y_{d_a}} d_a \quad (2.5b)$$

$$C_D = C_{D_0} + k_1 C_L + k C_L^2 \quad (2.5c)$$

¹That is, the aerodynamic force coefficients have to be multiplied by the force $\frac{1}{2}\rho V^2 S_{ref}$, where ρ is the air density, V is the total airspeed velocity and S_{ref} is a reference area to give the final forces. The moment coefficients have to be multiplied by $\frac{1}{2}\rho V^2 S_{ref} c_{ref}$ where c_{ref} is a reference length. The values of S_{ref} and c_{ref} for *each* coefficient **have** to be specified in the model description.

$$C_{\mathcal{L}} = C_{\mathcal{L}_{\beta}}\beta + C_{\mathcal{L}_{\dot{p}}}\frac{pb}{2V_{ref}} + C_{\mathcal{L}_{\dot{r}}}\frac{rb}{2V_{ref}} + C_{\mathcal{L}_{d_a}}d_a + C_{\mathcal{L}_{d_r}}d_r \quad (2.6a)$$

$$C_{\mathcal{M}} = C_{\mathcal{M}_0} + \boxed{C_{\mathcal{M}_{\alpha}}}\alpha + \boxed{C_{\mathcal{M}_{\dot{\alpha}}}}\frac{\dot{\alpha}\bar{c}}{2V_{ref}} + \boxed{C_{\mathcal{M}_{\dot{q}}}}\frac{q\bar{c}}{2V_{ref}} + \boxed{C_{\mathcal{M}_{d_p}}}\dot{d}_p \quad (2.6b)$$

$$C_{\mathcal{N}} = C_{\mathcal{N}_{\beta}}\beta + C_{\mathcal{N}_{\dot{p}}}\frac{pb}{2V_{ref}} + C_{\mathcal{N}_{\dot{r}}}\frac{rb}{2V_{ref}} + C_{\mathcal{N}_{d_a}}d_a + C_{\mathcal{N}_{d_r}}d_r \quad (2.6c)$$

Notice that in (2.5a) to (2.6c) each coefficient depends on some specific state variables and not all of them. The terms highlighted inside boxes are the ones affected by the internal movement of mass inside the aircraft due to load extraction manouvers, as described in 2.3.

2.1.3 Propulsion Forces and Moments

The total thrust force produced by the aircraft power system normally varies with flight regime. The two principal quantities on which this force depends are the airspeed velocity and air density. Depending on the type of engine used, there are different correlations for these variations, but those can be approximately summarized in a general equation of the form:

$$F = n_{eng}\pi F_{max} \left(\frac{\rho}{\rho_i}\right)^{n_p} \left(\frac{V}{V_i}\right)^{n_v} \quad (2.7)$$

Where:

n_{eng} is the number of engines

ρ_i is a reference air density

π is the throttle ($0 < \pi < 1$)

V_i is a reference airspeed

F_{max} is each engine's maximum force

n_ρ is a correlation exponent for density

ρ is the current air density

n_V is a correlation exponent for airspeed

V is the current airspeed

Once a suitable set of measurements (or theoretical model) are done with with (for) a given engine, equation (2.7) can be used to fit the data and give the thrust force for any desired flight regime. A typical value for n_ρ is 0.75 while n_V varies for the type of motor used. In the case of propeller driven aircraft n_V is -1, for turbofan engines n_V is 0 and for turbojet engines n_V is 1.

The propulsion forces will only produce moment if the axis of action of the thrust force does not pass through the aircraft's center of gravity. In that case, the moment produced will equal the cross product between the position vector of the engine with respect to C^* (\mathbf{p}^{eng/C^*}) and the thrust vector:

$$\mathcal{M}^{\mathcal{F}_p} = \mathbf{p}^{eng/C^*} \times \mathbf{F} \quad (2.8)$$

2.1.4 Attitude representations and Transformation Matrices

Euler Angles Due to their physical interpretation, the Euler angles are the most used set of parameters to perform coordinate transformations. If we have two frames completely independent of each other, as in figure 2.1, we can describe a transformation as three consecutive rotations, each about a different axis.

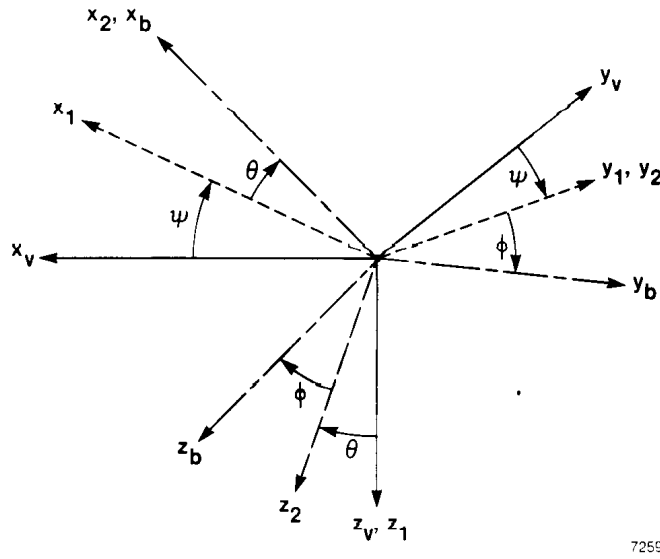


FIGURE 2.2 – Relationship between vehicle-carried vertical and body axis systems. (From reference (DUKE; ANTONIEWICZ; KRAMBEER, 1988))

Following figure 2.2, we first have the inertial (vehicle carried) reference frame \mathbf{V} . Rotating \mathbf{V} around the \mathbf{z}_V axis by an angle ψ , we get the intermediate frame $\mathbf{1}$. Next, rotating $\mathbf{1}$ around \mathbf{y}_1 an angle θ , we arrive at the second intermediate frame $\mathbf{2}$. Finally, rotating $\mathbf{2}$ around \mathbf{x}_2 an angle ϕ , we get the resulting body frame \mathbf{B} .

For a complete transformation, from \mathbf{V} - which we are calling $\mathbf{0}$ - to \mathbf{B} , we have:

$$\begin{bmatrix} x_0 \\ y_0 \\ z_0 \end{bmatrix} = \begin{bmatrix} \cos \theta \cos \psi & \cos \theta \sin \psi & -\sin \psi \\ \sin \phi \sin \theta \cos \psi & \sin \phi \sin \theta \sin \psi & \sin \phi \cos \theta \\ -\cos \phi \sin \psi & +\cos \phi \cos \psi & \\ \cos \phi \sin \theta \cos \psi & \cos \phi \sin \theta \sin \psi & \sin \phi \cos \theta \\ +\sin \phi \sin \psi & -\sin \phi \cos \psi & \end{bmatrix} \begin{bmatrix} x_V \\ y_V \\ z_V \end{bmatrix} \equiv \mathbf{T}_{0V} \mathbf{p}_V \quad (2.9)$$

Note that inverting the matrix \mathbf{T}_{0V} we can as well go from \mathbf{B} to $\mathbf{0}$. Verify also

(ROBINSON, 1958) that the transformation matrices are always orthogonal (i.e. $T^{-1} = T^T$). For our interest here, we can see that the Euler Angles can help us pass from any reference frame defined in subsection 2.1.1 to another, thus allowing us to write the equations of motion of the aircraft in terms of the angles which define each transformation.

As the Euler angles will be part of the state of our dynamical system, it is necessary to obtain the kinematics of frames that are moving in relation to each other. That is, suppose two reference frames, one fixed (i.e. $\mathbf{0}$) and another arbitrarily varying in time (i.e. \mathbf{B}). We want to relate the angular velocity of \mathbf{B} - written in \mathbf{B} - with the rates of change in time of the euler angles which define the transformation from $\mathbf{0}$ to \mathbf{B} .

To derive this relation, note that for each rotation implied in figure 2.2 we can associate an angular velocity vector ($\dot{\psi}$, $\dot{\theta}$ and $\dot{\phi}$). By writting these vectors in their own reference frames, we can use the transformations matrices to write them in the body reference frame. The result is the body angular velocity vector $\boldsymbol{\Omega}$.

Also, verify that each of these angular velocity vectors are always aligned with the axis around which the transformation is done (i.e. $\dot{\psi}$ is always aligned with \mathbf{z}_0), so they can be easily written in their original reference frames, allowing us to write:

$$\begin{aligned} \boldsymbol{\omega} &= \begin{bmatrix} \dot{\phi} \\ 0 \\ 0 \end{bmatrix} + \mathbf{T}_\phi \begin{bmatrix} 0 \\ \dot{\theta} \\ 0 \end{bmatrix} + \mathbf{T}_\phi \mathbf{T}_\theta \begin{bmatrix} 0 \\ 0 \\ \dot{\psi} \end{bmatrix} \\ \begin{bmatrix} p \\ q \\ r \end{bmatrix} &= \begin{bmatrix} \dot{\phi} - \sin \theta \dot{\psi} \\ \cos \phi \dot{\theta} + \sin \phi \cos \theta \dot{\psi} \\ -\sin \phi \dot{\theta} + \cos \phi \cos \theta \dot{\psi} \end{bmatrix} \end{aligned} \tag{2.10}$$

Finally, inverting (2.10):

$$\begin{bmatrix} \dot{\phi} \\ \dot{\theta} \\ \dot{\psi} \end{bmatrix} = \begin{bmatrix} p + (r \cos \phi + q \sin \phi) \tan \theta \\ q \cos \phi - r \sin \phi \\ (r \cos \phi + q \sin \phi) \sec \theta \end{bmatrix} \quad (2.11)$$

Equation 2.11 represents the Euler's angles dynamics for the general case of aircraft motion.

2.2 Longitudinal Equations of Motion

Considering the definitions of the auxiliary frames and remembering how the forces are written in their respective frames, we rewrite (2.2) as:

$$\mathbf{T}_{\alpha\beta} \begin{bmatrix} -D \\ Y \\ -L \end{bmatrix} + \mathbf{T}_{\alpha_f\beta_f} \begin{bmatrix} F \\ 0 \\ 0 \end{bmatrix} + \mathbf{T}_{\phi\theta\psi} \begin{bmatrix} 0 \\ 0 \\ mg \end{bmatrix} = m \begin{bmatrix} \dot{u} \\ \dot{v} \\ \dot{w} \end{bmatrix} + \dot{m} \begin{bmatrix} u \\ v \\ w \end{bmatrix} + \begin{bmatrix} p \\ q \\ r \end{bmatrix} \times m \cdot \begin{bmatrix} u \\ v \\ w \end{bmatrix} \quad (2.12a)$$

$$\mathbf{p}^{eng/C^*} \times \mathbf{T}_{\alpha_f\beta_f} \begin{bmatrix} F \\ 0 \\ 0 \end{bmatrix} + \begin{bmatrix} \mathcal{L} \\ \mathcal{M} \\ \mathcal{N} \end{bmatrix} = \mathbb{I} \cdot \begin{bmatrix} \dot{p} \\ \dot{q} \\ \dot{r} \end{bmatrix} + \dot{\mathbb{I}} \begin{bmatrix} p \\ q \\ r \end{bmatrix} + \begin{bmatrix} p \\ q \\ r \end{bmatrix} \times \mathbb{I} \cdot \begin{bmatrix} p \\ q \\ r \end{bmatrix} \quad (2.12b)$$

Where:

$\mathbf{T}_{\alpha\beta}$ is the transformation matrix from the aerodynamic to the body reference frame

$\mathbf{T}_{\alpha_f\beta_f}$ is the transformation matrix from the propulsion to the body reference frame

$\mathbf{T}_{\psi\theta\phi}$ is the transformation matrix from the topodetic to the body reference frame

Considering only the movement of the aircraft with leveled wing in the vertical plane - the so called longitudinal movement - we can cancel out (as in (ETKIN, 1972; ROSKAM, 2001)) the terms referring to the lateral and directional dynamics:

$$\beta_f = \beta = Y = \mathcal{L} = \mathcal{N} = p = r = v = \psi = \phi = 0 \quad (2.13)$$

Equations 2.12 are then simplified to:

$$\mathcal{M} + z_{F/CG} * F \cos(\alpha_f) = I_{yy}\dot{q} + \dot{I}_{yy}q \quad (2.14a)$$

$$-D \cos(\alpha) - L \sin(\alpha) + F \cos(\alpha_f) - mg \sin(\theta) = m\dot{u} + \dot{m}u + mqw \quad (2.14b)$$

$$-L \cos(\alpha) + D \sin(\alpha) - F \sin(\alpha_f) + mg \cos(\theta) = m\dot{w} + \dot{m}w - mqu \quad (2.14c)$$

Equations 2.14 can be solved for \dot{q} , \dot{u} and \dot{w} . As in the case of load extraction there is no continuous change of mass - only a discontinuous, sudden drop of weight - the term \dot{m} in the last two equations 2.14 can be neglected, giving:

$$\dot{q} = \frac{\mathcal{M} + z_{F/CG} * F \cos(\alpha_f) - \dot{I}_{yy}q}{I_{yy}} \quad (2.15a)$$

$$\dot{u} = \frac{1}{m} (-D \cos(\alpha) - L \sin(\alpha) + F \cos(\alpha_f) - mg \sin(\theta)) - qw \quad (2.15b)$$

$$\dot{w} = \frac{1}{m} (-L \cos(\alpha) + D \sin(\alpha) - F \sin(\alpha_f) + mg \cos(\theta)) + qu \quad (2.15c)$$

Furthermore, we have the kinematics equations for the attitude and position of the

aircraft on the vertical plane:

$$\dot{\theta} = q \quad (2.16a)$$

$$\dot{x} = u \cos \theta + w \sin \theta \quad (2.16b)$$

$$\dot{H} = -w \cos \theta + u \sin \theta \quad (2.16c)$$

It is usually found more useful for simulation and analysis purposes to exchange the body frame velocities u and w to the wind frame components V and α , through the relations:

$$u = V \cos \alpha \quad V = (u^2 + w^2)^{1/2}$$

$$w = V \sin \alpha \quad \alpha = \tan^{-1} \frac{u}{w}$$

To get:

$$\dot{q} = \frac{\boxed{\mathcal{M}} + z_{F/CG} F \cos(\alpha_f) - \boxed{\dot{I}_{yy}} q}{\boxed{I_{yy}}} \quad (2.17a)$$

$$\dot{V} = \frac{1}{\boxed{m}} \left(\boxed{-D} + F \cos(\alpha_f - \alpha) \right) - g \sin(\theta - \alpha) \quad (2.17b)$$

$$\dot{\alpha} = q - \frac{1}{\boxed{m} V} \left(\boxed{L} - \boxed{m} g \cos(\theta - \alpha) + F \sin(\alpha_f - \alpha) \right) \quad (2.17c)$$

$$\dot{\theta} = q \quad (2.17d)$$

$$\dot{x} = V \cos(\theta - \alpha) \quad (2.17e)$$

$$\dot{H} = V \sin(\theta - \alpha) \quad (2.17f)$$

Equations 2.17 represent the longitudinal dynamics of the aircraft. The terms highlighted inside boxes are the ones affected by the internal movement of mass inside the aircraft due to load extraction manouvers, as described in section 2.3.

2.3 Effects of internal mass displacement on aircraft dynamics

The dynamics of the aircraft are affected by the displacement of an internal load as it changes the center of gravity location from its original position.

Thus, all the variables from the aircraft dynamics dependent on CG position - the ones highlighted by boxes in equations 2.5, 2.6 and 2.17 - have to be corrected by the current CG position. These corrections are presented below.

Variation of I_{yy} and \dot{I}_{yy} The moment of inertia of the airplane carrying a load can be expressed as the sum of both the airplane and load inertias with respect to the current *C.G.* location:

$$I_{yy}^{Total/X_{cg}} = I_{yy}^{A/X_{cg}} + I_{yy}^{C/X_{cg}} \quad (2.18)$$

Each of the terms on the right-hand side of equation 2.18 can be further expressed as the sum of the moment of inertia of each component with respect to its own *C.G.* with the product of its mass to the square of the distance from its *C.G.* to the *C.G.* of the complete system. Defining X_{cg0} as the center of mass of the unloaded aircraft and X_{cgC} as the position of the load's center of mass we can write:

$$I_{yy}^{Total/X_{cg}} = I_{yy}^{A/X_{cg0}} + (X_{cg} - X_{cg0})^2 m_A + I_{yy}^{C/X_{cgC}} + (X_{cg} - X_{cgC})^2 m_C \quad (2.19)$$

The term $I_{yy}^{C/X_{cgC}}$ in equation 2.19 is considered negligible with relation to the others. The displacement of the center of gravity of the loaded airplane with respect to its orig-

inal location ($X_{cg} - X_{cg0}$) will appear in other expressions as well, which motivates the definition:

$$\Delta X_{cg} \triangleq X_{cg} - X_{cg0} \quad (2.20)$$

The current position of center of gravity of the aircraft at a given time is expressed as:

$$X_{cg} = \frac{X_{cg0}m_A + X_{cgC}m_C}{m_A + m_C} \quad (2.21)$$

Defining the *aircraft load-mass ratio* as $\mu_A \triangleq m_A/(m_A + m_C)$, the relation ($X_{cg} - X_{cgC}$) can be expressed as:

$$(X_{cg} - X_{cgC}) = \frac{-\mu_A}{(1 - \mu_A)}(X_{cg} - X_{cg0}) = \frac{-\mu_A}{(1 - \mu_A)}\Delta X_{cg} \quad (2.22)$$

Substituting equations 2.20 and 2.22 in equation 2.19 we find:

$$\boxed{I_{yy} = I_{yy0} + \frac{m_A}{1 - \mu_A}\Delta X_{cg}^2} \quad (2.23)$$

Where the inertia of the empty plane $I_{yy}^{A/X_{cg0}}$ was represented as I_{yy0} . The derivative of the inertia with respect to time is obtained directly from equation 2.23 and is given by:

$$\boxed{\dot{I}_{yy} = \frac{2m_A}{1 - \mu_A}\Delta X_{cg}\Delta \dot{X}_{cg}} \quad (2.24)$$

Variation of C_{M_α} Taking the definitions of figure 2.3 as a base to calculate the balance of longitudinal forces and moments acting on the aircraft, one arrives at equation 2.25 for the dependence of the pitching moment with the angle of attack (ROSKAM, 2001;

by imposing that $C_{\mathcal{M}_\alpha}|_{N.P.} = 0$. So, re-writting 2.25 for the neutral point one gets:

$$\bar{X}_N = \frac{C_{L_{\alpha wf}} \bar{X}_{ac wf} + C_{L_{\alpha h}} \eta_h \frac{S_h}{S} (1 - \frac{d\epsilon}{d\alpha}) \bar{X}_{ac h}}{C_{L_{\alpha wf}} + C_{L_{\alpha h}} \eta_h \frac{S_h}{S} (1 - \frac{d\epsilon}{d\alpha})} \quad (2.26)$$

Defining:

$$C_{L_{\alpha h}}' \triangleq C_{L_{\alpha h}} \eta_h \frac{S_h}{S} (1 - \frac{d\epsilon}{d\alpha}) \quad (2.27)$$

And substituting 2.26 and 2.27 in 2.25 one finds:

$$C_{\mathcal{M}_\alpha}|_{X_{cg}} = \underbrace{(C_{L_{\alpha wf}} + C_{L_{\alpha h}}')}_{C_{L_\alpha}} (\bar{X}_{cg} - \bar{X}_N) \quad (2.28)$$

Finally, substituting \bar{X}_{cg} in 2.28 for $\bar{X}_{cg0} + \Delta \bar{X}_{cg}$ we find the formula for the correction of the derivative of $C_{\mathcal{M}_\alpha}$ with *C.G.* displacement:

$$\boxed{C_{\mathcal{M}_\alpha}|_{X_{cg}} = C_{\mathcal{M}_\alpha}|_{X_{cg0}} + C_{L_\alpha} \Delta \bar{X}_{cg}} \quad (2.29)$$

Variation of $C_{\mathcal{M}_{d_p}}$ Referring again to figure 2.3 one expresses the variation of pitching moment with elevator position as (ROSKAM, 2001). After substitution the same substitution for \bar{X}_{cg} done before:

$$\boxed{C_{\mathcal{M}_{d_p}}|_{X_{cg}}} = - \underbrace{C_{L_{\alpha h}} \eta_h \tau_e \frac{S_h}{S}}_{C_{L_{d_p}}} (\bar{X}_{ac h} - \bar{X}_{cg}) = \boxed{C_{\mathcal{M}_{d_p}}|_{X_{cg0}} + C_{L_{d_p}} \Delta \bar{X}_{cg}} \quad (2.30)$$

Variation of $C_{L_{\hat{q}}}$ and $C_{\mathcal{M}_{\hat{q}}}$ When the aeroplane undergoes a sudden pitch variation, the angle of attack of the horizontal tail is modified by (ROSKAM, 2001; ETKIN, 1972):

$$\Delta\alpha = \frac{q(X_{ac_h} - X_{cg})}{V_0} \quad (2.31)$$

This corresponds to an increase in lift:

$$\Delta L = \frac{1}{2}\rho V_0^2 S_h \eta_h C_{L_{\alpha h}} \frac{q(X_{ac_h} - X_{cg})}{V_0} \quad (2.32)$$

Dividing 2.32 by $\frac{1}{2}\rho V_0^2 S$ one finds:

$$\Delta C_L = \underbrace{2C_{L_{\alpha h}} \eta_h \frac{S_h}{S} (\bar{X}_{ac_h} - \bar{X}_{cg})}_{C_{L_{\hat{q}}}} \underbrace{\left(\frac{q\bar{c}}{2V_0} \right)}_{\hat{q}} \quad (2.33)$$

Thus the variation of $C_{L_{\hat{q}}}$ with ΔX_{cg} is given by:

$$C_{L_{\hat{q}}}|_{X_{cg}} = C_{L_{\hat{q}}}|_{X_{cg0}} - \frac{C_{L_{\hat{q}}}|_{X_{cg0}}}{(\bar{X}_{ac_h} - \bar{X}_{cg0})} \Delta \bar{X}_{cg} \quad (2.34)$$

As for the derivative $C_{\mathcal{M}_{\hat{q}}}$, it is simply the negative of the product of $C_{L_{\hat{q}}}$ with $(\bar{X}_{ac_h} - \bar{X}_{cg})$:

$$C_{\mathcal{M}_{\hat{q}}}|_{X_{cg}} = -2.2C_{L_{\alpha h}} \eta_h \frac{S_h}{S} (\bar{X}_{ac_h} - \bar{X}_{cg})^2 \quad (2.35)$$

Where a factor of 10% was added to take into account the effect of the wing on the pitching moment. This is called the *fudge-factor* (ROSKAM, 2001). Using 2.34 and 2.35

one can solve for the horizontal tail distance from the center of mass:

$$(\bar{X}_{ac_h} - \bar{X}_{cg0}) = \frac{C_{\mathcal{M}_{\hat{q}}}|_{X_{cg0}}}{-1.1C_{L_{\hat{q}}}|_{X_{cg0}}} \quad (2.36)$$

Substituting 2.36 in equations 2.34 and 2.35 one finds:

$$C_{L_{\hat{q}}}|_{X_{cg}} = C_{L_{\hat{q}}}|_{X_{cg0}} + \frac{1.1(C_{L_{\hat{q}}}|_{X_{cg0}})^2}{C_{\mathcal{M}_{\hat{q}}}|_{X_{cg0}}} \Delta \bar{X}_{cg} \quad (2.37)$$

$$C_{\mathcal{M}_{\hat{q}}}|_{X_{cg}} = C_{\mathcal{M}_{\hat{q}}}|_{X_{cg0}} + 2.2C_{L_{\hat{q}}}|_{X_{cg0}} \Delta \bar{X}_{cg} + \frac{(1.1C_{L_{\hat{q}}}|_{X_{cg0}})^2}{C_{\mathcal{M}_{\hat{q}}}|_{X_{cg0}}} (\Delta \bar{X}_{cg})^2 \quad (2.38)$$

Variation of $C_{\mathcal{M}_{\hat{\alpha}}}$ As in the case of the $C_{\mathcal{M}_{\hat{q}}}$ derivative, $C_{\mathcal{M}_{\hat{\alpha}}}$ is the negative product of $C_{L_{\hat{\alpha}}}$ with the distance from the horizontal tail with the $C.G.$.

This effect is caused mainly by the variation in intensity of the vortices shed by the wing with instantaneous angle of attack. The vortices shed by the wing at a time t will reach the horizontal tail at a time $t + \Delta t$, where Δt is the time the flow takes to get from the wing to the horizontal tail. This delay is a function of the aircraft's speed and geometric properties, as the distance from the aerodynamic centers of the wing and horizontal tail. There is a common practical approximation in the literature (ROSKAM, 2001; ETKIN, 1972) where this distance is approximated by the distance from the $C.G.$ to the horizontal tail. While this is a valid approximation for most flight conditions, this is not true in our case.

One can find in the cited references a more in depth description of the calculations for the derivatives $C_{L_{\hat{\alpha}}}$ and $C_{\mathcal{M}_{\hat{\alpha}}}$. We only stress here that $C_{L_{\hat{\alpha}}}$ does **not** depend on

the aircraft's center of mass on a first approximation. It only depends on the geometric properties of the aeroplane.

The dependence of $C_{\mathcal{M}_{\hat{\alpha}}}$ with the $C.G.$ position is thus given by:

$$\boxed{C_{\mathcal{M}_{\hat{\alpha}}}|_{X_{cg}} = -C_{L_{\hat{\alpha}}}(\bar{X}_{ac_h} - \bar{X}_{cg}) = C_{\mathcal{M}_{\hat{\alpha}}}|_{X_{cg0}} + C_{L_{\hat{\alpha}}}\Delta\bar{X}_{cg}} \quad (2.39)$$

2.4 Summary

Recollecting the development of this chapter, we may now state the dynamics of the longitudinal motion for a rigid aircraft with variable longitudinal $C.G.$ position and variable longitudinal inertia, as expected for the case of a load extraction manouver.

The dynamics is given by the system of ordinary differential equations (2.17):

$$\begin{aligned} \dot{q} &= \frac{\boxed{\mathcal{M}} + z_{F/CG}F \cos(\alpha_f) - \boxed{\dot{I}_{yy}}q}{\boxed{I_{yy}}} \\ \dot{V} &= \frac{1}{\boxed{m}} \left(\boxed{-D} + F \cos(\alpha_f - \alpha) \right) - g \sin(\theta - \alpha) \\ \dot{\alpha} &= q - \frac{1}{\boxed{m}V} \left(\boxed{L} - \boxed{m}g \cos(\theta - \alpha) + F \sin(\alpha_f - \alpha) \right) \\ \dot{\theta} &= q \\ \dot{x} &= V \cos(\theta - \alpha) \\ \dot{H} &= V \sin(\theta - \alpha) \end{aligned}$$

The aerodynamic forces and moment are given by:

$$L = \frac{1}{2}\rho V^2 C_L \quad D = \frac{1}{2}\rho V^2 C_D \quad \mathcal{M} = \frac{1}{2}\rho V^2 \bar{c} C_{\mathcal{M}}$$

The aerodynamic coefficients $(C_L, C_{\mathcal{M}})$, can be reasonably well aproximated to depend linearly on the state variables as in equations (2.5) and (2.6). The drag coefficient C_D is normally aproximated as a parabolic function of the lift coefficient:

$$\begin{aligned} C_L &= C_{L_0} + C_{L_\alpha} \alpha + \boxed{C_{L_{\hat{q}}}} \frac{q\bar{c}}{2V_{ref}} + C_{L_{d_p}} d_p \\ C_D &= C_{D_0} + k_1 C_L + k C_L^2 \\ C_{\mathcal{M}} &= C_{\mathcal{M}_0} + \boxed{C_{\mathcal{M}_\alpha}} \alpha + \boxed{C_{\mathcal{M}_{\dot{\alpha}}}} \frac{\dot{\alpha}\bar{c}}{2V_{ref}} + \boxed{C_{\mathcal{M}_{\hat{q}}}} \frac{q\bar{c}}{2V_{ref}} + \boxed{C_{\mathcal{M}_{d_p}}} d_p \end{aligned}$$

All the boxed terms in the above equations are dependent on the aircraft's *C.G.* location as varied by the displacement of the cargo load. This dependence is given by equations (2.23)-(2.24), (2.29)-(2.30) and (2.37)-(2.39):

$$\begin{aligned} I_{yy} &= I_{yy0} + \frac{m_A}{1 - \mu_A} \Delta X_{cg}^2 \\ \dot{I}_{yy} &= \frac{2m_A}{1 - \mu_A} \Delta X_{cg} \Delta \dot{X}_{cg} \\ C_{\mathcal{M}_\alpha} &= C_{\mathcal{M}_\alpha}|_{X_{cg0}} + C_{L_\alpha} \Delta \bar{X}_{cg} \\ C_{\mathcal{M}_{d_p}} &= C_{\mathcal{M}_{d_p}}|_{X_{cg0}} + C_{L_{d_p}} \Delta \bar{X}_{cg} \\ C_{L_{\hat{q}}} &= C_{L_{\hat{q}}}|_{X_{cg0}} + \frac{1.1(C_{L_{\hat{q}}}|_{X_{cg0}})^2}{C_{\mathcal{M}_{\hat{q}}}|_{X_{cg0}}} \Delta \bar{X}_{cg} \\ C_{\mathcal{M}_{\hat{q}}} &= C_{\mathcal{M}_{\hat{q}}}|_{X_{cg0}} + 2.2 C_{L_{\hat{q}}}|_{X_{cg0}} \Delta \bar{X}_{cg} + \frac{(1.1 C_{L_{\hat{q}}}|_{X_{cg0}})^2}{C_{\mathcal{M}_{\hat{q}}}|_{X_{cg0}}} (\Delta \bar{X}_{cg})^2 \\ C_{\mathcal{M}_{\dot{\alpha}}} &= -C_{L_{\dot{\alpha}}} (\bar{X}_{ac_h} - \bar{X}_{cg}) = C_{\mathcal{M}_{\dot{\alpha}}}|_{X_{cg0}} + C_{L_{\dot{\alpha}}} \Delta \bar{X}_{cg} \end{aligned}$$

Taken together, the equations just stated define the desired dynamic model.

3 Nonlinear Control

3.1 Feedback Linearization

Feedback linearization was one the first nonlinear control methods to be applied in aircraft control and for some time remained the paradigm of nonlinear controllers applied to aeronautical problems. We will find in the aeronautical literature the name of *Dynamic Inversion* for this method. The idea behind feedback linearization (SLOTINE; LI, 1991; ISIDORI, 1995) is to change the state variables through a coordinate transformation $\mathbf{Z} = \mathbf{Z}(X)$ (a diffeomorphism in a certain domain Ω of \mathbb{R}^n) and to use a control $u = u(X, v)$ so that the new system $[\mathbf{Z}, v]$ is linear or at least partially linear in the new set of coordinates, and that the new control variable v can drive the system to a desired trajectory.

The application of the theory of feedback linearization to the control of aircraft's attitude will be explored. By aircraft piloting, we will be referring to the process of keeping a desired orientation, which are reflected in the equations by the euler angles. This is also called the aircraft *fast dynamics* as in opposite to the usually slower dynamics of the aircraft's velocity.

The advantage of choosing the euler angles as output variables, as it will be seen, is that a relatively easy implementation of dynamic inversion can be performed. On the

other hand, one has to keep in mind that the wind angles (α, β) cannot fall out of a certain domain to keep the validity of the equations used.

3.1.1 The SISO Case

Let us begin the development by considering a system of the form:

$$\begin{cases} \dot{X} = f(X) + g(X)u & X \in \mathbb{R}^n \quad u \in \mathbb{R} \\ y = h(X) & y \in \mathbb{R} \end{cases} \quad (3.1)$$

And let $\Omega \subset \mathbb{R}^n$ be the domain of interest. This is a system with a **Single Input** u and a **Single Output** y . Lets take the derivative of y with respect to time to obtain:

$$\dot{y} = \nabla h \cdot \dot{X} = \nabla h \cdot (f(X) + g(X)u) \quad (3.2)$$

Now, if $\nabla h \cdot g(X)$ is zero for all $X \in \Omega$, $\Omega \subset \mathbb{R}^n$, we have to continue to derivate (3.2) in order for the control u to appear. To simplify the notation, before we continue, lets introduce the so called *Lie Derivatives* ([ISIDORI, 1995](#)).

Definition 1 *Let $h: \mathbb{R}^n \rightarrow \mathbb{R}$ be a smooth scalar function and $\mathbf{f}: \mathbb{R}^n \rightarrow \mathbb{R}^n$ be a smooth vector field on \mathbb{R}^n . Then the Lie Derivative of h with respect to \mathbf{f} is a scalar function defined by: $L_f h \equiv \nabla h \cdot \mathbf{f}$*

Repeated Lie Derivatives can be defined recursively as follows:

$$\begin{aligned} L_f^0 h &= h \\ L_f^i h &= L_f L_f^{i-1} h = \nabla (L_f^{i-1} h) \cdot \mathbf{f} \quad i = 1, 2, \dots \end{aligned}$$

With the definition above we can write (3.2) as:

$$\dot{y} = L_f h + L_g h u$$

And then, in the considered case of $L_g h = 0$ for all $X \in \Omega$, we derivate (3.2) again:

$$\ddot{y} = L_f^2 h + L_g L_f h u \quad (3.3)$$

If $L_g L_f h = 0$ for all $X \in \Omega$ we continue to derivate until:

$$y^{(r)} = L_f^r h + L_g L_f^{r-1} h u; \quad L_g L_f^{r-1} h \neq 0 \text{ for some } X \in \Omega \quad (3.4)$$

When a system as (3.1) has an output that can be written in the form (3.4) we call the number r the *relative degree* of the system.

Suppose the relative degree r is equal to the state dimension n . In this case, consider the subset of Ω , Ω' which consists of all the points X' where $L_g L_f^{r-1} h \neq 0$. In Ω' , consider the following control law:

$$\begin{aligned} u &= [L_g L_f^{r-1} h]^{-1} (v - L_f^r h) \\ v &= y_d^{(r)} - \sum_{i=0}^{r-1} k_i (y^{(i)} - y_d^{(i)}) \end{aligned} \quad (3.5)$$

such that the coefficients k_i are chosen so that the roots of the polynomial:

$$\mu(\lambda) = \lambda^r + \sum_{i=0}^{r-1} k_i \lambda^i$$

will all have negative real part.

Note the controller scheme as presented in figure 3.1. As we can see, that are two feedback signals. One is to generate the error with respect to the desired trajectory and the other is to cancel the plants nonlinearities (also called the linearization loop (STEVENS; LEWIS, 2003)).

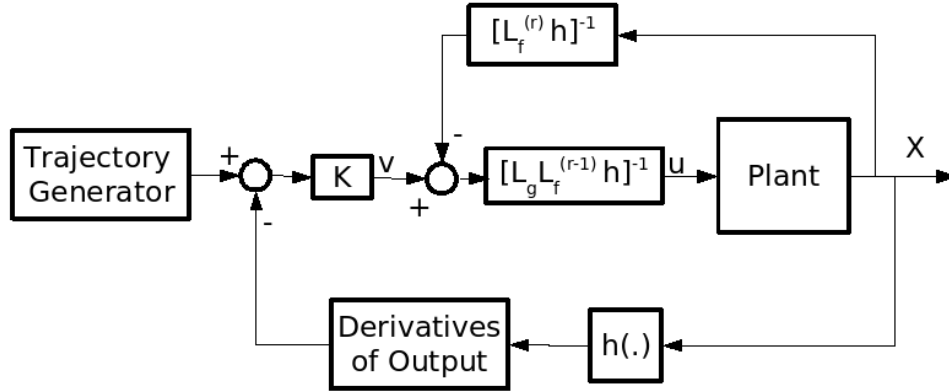


FIGURE 3.1 – The feedback linearization controller block diagram scheme.

We can see that (3.5) will drive the output to follow a desired trajectory $y_d(t)$, because by substituting (3.5) in (3.4), and defining the *error* as $e(t) \equiv y(t) - y_d(t)$ we get:

$$e^{(r)} + \sum_{i=1}^{r-1} k_i e^{(i)} = 0$$

and considering the choice of k_i we have that $e \rightarrow 0$ when $t \rightarrow \infty$ and thus the output trajectory becomes the same as the desired trajectory.

3.1.1.1 The Normal Form

For case considered so far, with relative degree equal to the state dimension ($r = n$) it was presented one choice of control that can drive the output in the desired way, but nothing was said about the rest of the state variables. Now, there are two possibilities to consider: $r = n$ and $r < n$ (r can never be greater than n for systems of the form (3.1),

([SLOTINE; LI, 1991](#))). In the first case ($r = n$), we can define a coordinate transformation

$\mathbf{Z} = \mathbf{Z}(X)$:

$$\mathbf{Z} = \begin{bmatrix} h \\ L_f h \\ L_f^2 h \\ \vdots \\ L_f^{r-1} h \end{bmatrix}$$

and use control $u = u(X, v)$ with u defined in (3.5) to write the new system as:

$$\begin{aligned} \dot{\mathbf{Z}} &= A\mathbf{Z} + bv \\ \text{Where: } A &= \begin{bmatrix} 0 & 1 & 0 & \cdots & 0 \\ 0 & 0 & 1 & \cdots & 0 \\ \vdots & \vdots & \vdots & \ddots & \vdots \\ 0 & \cdots & \cdots & 0 & 1 \\ 0 & \cdots & \cdots & 0 & 0 \end{bmatrix} \quad \text{and } b = \begin{bmatrix} 0 \\ 0 \\ \vdots \\ 0 \\ 1 \end{bmatrix} \end{aligned} \quad (3.6)$$

In this case, \mathbf{Z} is called the *linearizing state* and (3.5) is called the *linearizing control law* ([SLOTINE; LI, 1991](#)). Also (3.6) is called the **normal form** of a system whose relative degree r equals the dimension of the state vector (n). The normal form allow us to observe more directly the dynamics obtained by feedback linearization of a system, as it can be noticed by the simplicity of the dynamics written in the new variables.

Now we follow to the case when $r < n$. Let $\mathbf{Z} = [h, L_f h, \dots, L_f^{r-1} h]^T$. As $\dim(\mathbf{Z}) = r$, we have to complete the state transformation with a vector \mathbf{W} such that $\dim(\mathbf{W}) = n - r$.

The normal form in this case will be written as:

$$\dot{\mathbf{Z}} = \begin{bmatrix} L_f h \\ L_f^2 h \\ \vdots \\ L_f^{r-1} h \\ \alpha(\mathbf{Z}, \mathbf{W}) + \beta(\mathbf{Z}, \mathbf{W})u \end{bmatrix} \quad \dot{\mathbf{W}} = \psi(\mathbf{Z}, \mathbf{W}) \quad (3.7)$$

with the output written as $y = Z_1$.

The new state variables \mathbf{Z} and \mathbf{W} are called the *normal coordinates* of the system in the domain Ω' where the transformation is valid. Of course, we would have to prove that first, it exists a coordinate transformation of the form (3.7) where \mathbf{Z} and \mathbf{W} are the new state; then, that this transformation is indeed a local *diffeomorphism*. We will not deal with this matter here, please refer to (SLOTINE; LI, 1991; ISIDORI, 1995).

Zero Dynamics When proving that \mathbf{Z} and \mathbf{W} form a local diffeomorphism in the domain Ω' it is also noticed the interesting fact that the vector \mathbf{W} form a part of the state that is unobservable by the control u . That is, writing $\mathbf{W} = [\psi_1(X), \dots, \psi_{n-r}(X)]^T$, it is proved that $\nabla \psi_i g = 0$ for $i = 1, \dots, n - r$. The practical consequence is that no matter what we try with the command u , when $r < n$, there will always be a part of the state over which we will not be able to “reach”.

This part of the state is called the *zero dynamics*. That is because if we adjust the control u in (3.7) to cancel out all the components of the \mathbf{Z} normal coordinates part, the output will be guaranteed to continue zero. On the other hand, nothing is known about the evolution of the internal variables in \mathbf{W} .

The zero dynamics plays a very important role when applying the method of feedback linearization, once it has to be guaranteed stable. To study the dynamic behavior of the zero dynamics, methods of Lyapunov analysis can be used (see section 3.2). If this part of the state is discovered to be unstable, a different choice of output must be selected (SLOTINE; LI, 1991; STEVENS; LEWIS, 2003).

3.1.2 The MIMO Case

The procedure for feedback linearization of Multiple Input, Multiple Output nonlinear systems is analogous to the SISO case. Lets consider the system (3.1). Differentiating output y_i for r_i times until at least one of the inputs appears in the equation for y_i we have:

$$y_i^{(r_i)} = L_f^{r_i} h_i + \sum_{j=1}^m (L_{g_j} L_f^{r_i-1} h_i u_j) \quad (3.8)$$

Where : $L_{g_j} L_f^{r_i-1} h_i \neq 0$ for at least one j in Ω'_i

Performing the same procedure for all the outputs, we can write:

$$\begin{bmatrix} y_1^{(r_1)} \\ \vdots \\ y_m^{(r_m)} \end{bmatrix} = \begin{bmatrix} L_f^{r_1} h_1 \\ \vdots \\ L_f^{r_m} h_m \end{bmatrix} + \mathbf{E}(X) u \quad (3.9)$$

Where : $\mathbf{E}_{i,j} = L_{g_j} L_f^{r_i-1} h_i \quad i, j = 1, \dots, m$

Now, let Ω^T be the intersection of all the sets Ω'_i . If \mathbf{E} is invertible in Ω^T then we can

choose the control:

$$u = \mathbf{E}^{-1} \begin{bmatrix} v_1 - L_f^{r_1} h_1 \\ \vdots \\ v_m - L_f^{r_m} h_m \end{bmatrix} \quad (3.10)$$

Obtaining the equations $y_i^{(r_i)} = v_i$. Finally, we choose v_i to make the system converge to each desired trajectory $y_{id}(t)$.

The number $r = \sum_{j=1}^m r_j$ is called the *total relative degree* of the system (3.1). The definitions for zero dynamics can be extended also to the MIMO case. When \mathbf{E} is a singular matrix in some point of the domain of interest, the outputs have to be modified or the output has to be sequentially differentiated to obtain a new system where \mathbf{E} is invertible (SLOTINE; LI, 1991).

To clarify the procedure, the next sections this exact procedure will be applied to the euler angle dynamics of the aircraft.

3.1.3 Summary of the theory

The application to feedback linearization to aircraft control can bring a good number of advantages. For instance, the simulated controller code can be programmed directly in the avionics of the aircraft, with no needs for look up tables or gain scheduling, once this controller can perform equally in any flight condition. This method can also be used both by stabilizing and tracking problems in severe, large amplitude manoeuvres, as long as the physical description of the aircraft remain the same.

It also naturally has some important limitations. In the case of aircraft control, we can emphasize two inconveniences:

- We have to measure the entire state to use the controller. This is not easy from a practical point of view and can get specially hard in the case of nonlinear systems, where observers are harder to construct and the convergence of the coupling between the observer and the control system may not always be proofed.
- We need a complete, precise model of the system dynamics. Although it is possible to have a fair description of the airplane dynamics (see chapter 2), the values used are not always (normally never) known precisely enough, due to environment perturbations, fabrication defects or just a simplified analysis of the system. The not so well modelled dynamics can not be accounted for in a formal fashion in the case of feedback linearization (robustness issues (SLOTINE; LI, 1991)), but there are ways of trying to solve this problem, as the adaptive control schemes (section 4).

3.2 Lyapunov Analysis of Nonlinear Systems

In this subsection we will deal first with *Autonomous Systems*, that is, systems whose description and parameters do not vary with time. After the major results are extended to the case of *Non-Autonomous Systems* which is the case of the airplane (it burns fuel, deploys the landing gear, deflects high lift surfaces, etc) and also the case when, even considering the airplane an autonomous system for a given flight condition, adaptive control methods are used.

Consider then the following nonlinear time-invariant system:

$$\dot{X} = \mathbf{f}(X); \quad \mathbf{x}(0) = \mathbf{x}_0 \quad (3.11)$$

Let $\mathbf{x}(t)$ be a solution and \mathbf{x}_e be an equilibrium point of (3.11) (i.e. $\mathbf{f}(\mathbf{x}_e) = \mathbf{0}$).

Definitions Lets list a set of definitions necessary to well pose the theorem of Lyapunov's direct method and the invariant set theorem (LaSalle's theorem) which together form a powerful tool of analysis of stability for nonlinear autonomous systems.

Definition 2 If $\mathbf{f}(X)$ is a continuous function in \mathbf{x}_e and there exists a strictly positive real number L such that:

$$\| \mathbf{f}(X_1) - \mathbf{f}(X_2) \| \leq L \| X_1 - X_2 \|$$

For all X_1 and X_2 in a finite neighborhood of \mathbf{x}_e then \mathbf{f} is said to be **locally Lipschitz** in x_e .

Definition 3 $\mathbf{x}(t)$ is **bounded** if there exists a non-negative constant $\gamma(\mathbf{x}(t))$ such that:

$$\| \mathbf{x}(t) \| \leq \gamma(\mathbf{x}(t)), \quad \forall t \geq 0$$

Definition 4 \mathbf{x}_e is **stable** if $\forall \epsilon > 0$ there exists $\delta(\epsilon) > 0$ such that:

$$\| x(0) - x_e \| < \delta(\epsilon) \Rightarrow \| x(t) - x_e \| < \epsilon \quad \forall t \geq 0$$

And \mathbf{x}_e is **unstable** when not stable.

Definition 5 \mathbf{x}_e is **attractive** if there exists a non-negative real function $\mathbf{r}(\mathbf{x}(t))$ such that:

$$\| x(0) - x_e \| \leq \mathbf{r}(\mathbf{x}(t)) \Rightarrow \lim_{t \rightarrow \infty} \| x(t) - x_e \| \rightarrow 0$$

In this case, we can define a subset Ω of \mathbb{R}^n such that $\mathbf{x}_e \in \Omega$ and that every $\mathbf{X}(0) \in \Omega$ will produce a trajectory such that $\lim_{t \rightarrow \infty} \|\mathbf{x}(t) - \mathbf{x}_e\| \rightarrow 0$. Then, Ω is called **the domain of attraction** of \mathbf{x}_e

Definition 6 \mathbf{x}_e is (locally) **asymptotically stable (AS)** if it is **stable** and **attractive**.

Definition 7 \mathbf{x}_e is **globally asymptotically stable (GAS)** if it is **stable** and **attractive** for all $\mathbf{X}(0)$. That is, the **the domain of attraction** of \mathbf{x}_e is the whole \mathbb{R}^n .

Definition 8 A scalar field $V : \mathbb{R}^n \rightarrow \mathbb{R}_+$ is said to be **positive (semi-) definite** in a ball $B_{R_{X_e}}$ if:

$$\text{If } X \neq X_e \Rightarrow V(X) > 0 \quad (V(X) \geq 0) \quad \forall X \in \mathbb{R}^n$$

And **negative (semi-) definite** if $-V(X)$ is **positive (semi-) definite**.

Definition 9 A scalar field $V : \mathbb{R}^n \rightarrow \mathbb{R}_+$ is **radially unbounded** if:

$$\|V(X)\| \rightarrow \infty \quad \text{when} \quad \|X\| \rightarrow \infty$$

Definition 10 $G \subset \mathbb{R}^n$ is said to be an **invariant set** of a dynamical system if all the trajectories of the system starting in G remain in G for all future time.

Now we are ready to define the theorems:

Theorem 1 (Lyapunov's direct method) Let \mathbf{x}_e be a equilibrium point of (3.11) and $\mathbf{f}(X)$ be locally Lipschitz in x_e . Let $V : \mathbb{R}^n \rightarrow \mathbb{R}$ have continuous first partial derivatives, be positive definite and radially unbounded. In such conditions:

- x_e is globally stable (GS), if $\dot{V}(X)$ is negative semi-definite.

- x_e is globally asymptotically stable (GAS), if $\dot{V}(X)$ is negative definite.

Theorem 2 (LaSalle’s invariant set theorem) Consider the system in (3.11), with $f(X)$ a continuous function. Let $V : \mathbb{R}^n \rightarrow \mathbb{R}$ have/be:

- continuous first partial derivatives
- positive definite
- radially unbounded
- $\dot{V}(X)$ is negative semi-definite

Let also Ω be the set of all points in \mathbb{R}^n where $\dot{V}(X) = 0$.

If M is the largest invariant set in Ω , then all the trajectories of (3.11) asymptotically converge to M .

The proofs of these theorems can be found in (SLOTINE; LI, 1991; KHALIL, 2002; ISIDORI, 1995). ■

3.3 Lyapunov’s direct method and Backstepping

The Backstepping Method is derived directly from the study of the *Lyapunov’s Direct Method*, a general method for finding stability properties of nonlinear dynamic systems, and its extensions. According to (FOSSEN; STRAND, 1998), it is a *recursive* design methodology for finding both the feedback control laws and *Lyapunov Functions* in a systematic manner.

Historically, the idea of the integrator backstepping has been developed in the end of the decade of 1980 (FOSSSEN; STRAND, 1998) and soon developed to cascaded systems analysis, which permitted the design of complete nonlinear systems that could be put in an specific form: *the strict feedback form*.

One good advantage of Lyapunov Analysis, an thus backstepping design, is that it allows one to use physical properties of a system, as dissipation of energy, natural damping or potential force fields, in advantage of the controller, thus ignoring “good” nonlinearities, that is, characteristics of the system that are inherently stable, and focusing the control effort where it is really needed, that is, in that part of the dynamics which is not naturally stable (FOSSSEN; STRAND, 1998; HARKEGARD, 2001b; HARKEGARD, 2001a).

3.3.1 Extension to non-autonomous systems

Lets now generalize the results obtained above for the case of non-autonomous systems, that is, for systems that when written in the form (3.11) will have a function of the form $\mathbf{f}(X, t)$ to describe its dynamics. This includes the systems whose equations can change its parameters with time. We will be interested naturally with smooth changes, or more precisely, with continuous functions $\mathbf{f}(X, t)$ such that $\frac{\partial}{\partial t}\mathbf{f}(X, t)$ is also continuous.

Definition 11 A function $f : \mathbb{R} \rightarrow \mathbb{R}$ is said to be **uniformly continuous** if:

$$\forall \delta > 0, \exists \epsilon(\delta) > 0 | \forall x, x_0 \in \mathbb{R}, \|x - x_0\| < \epsilon \Rightarrow \|f(x) - f(x_0)\| < \delta$$

Lemma 1 (Barballat’s Lemma) If the differentiable function $f(t)$ has a finite limit as $t \rightarrow \infty$ and $\dot{f}(t)$ is uniformly continuous then $\lim_{t \rightarrow \infty} \dot{f}(t) = 0$

Theorem 3 Let $V : \mathbb{R}^n \times \mathbb{R} \rightarrow \mathbb{R}$ be a continuous scalar field $V(X(t), t)$, have continuous

first partial derivatives and be such that:

- $V(x, t)$ is lower bounded
- $\dot{V}(x, t)$ is negative semi-definite
- $V(x, t)$ is radially unbounded

Then $\dot{V}(x, t) \rightarrow 0$ as $t \rightarrow \infty$.

Moreover, in the case of a dynamic system $\dot{X} = \mathbf{f}(X, t)$, if a function $V(X(t), t)$ is found and have the properties above, it approaches a finite limit V_∞ when $t \rightarrow \infty$ and $V_\infty \leq V(X(0), 0)$. Any trajectory of the system will then be globally uniformly bounded if $\dot{V}(X, t)$ is negative semi-definite and will have a globally asymptotically stable equilibrium point if $\dot{V}(X, t)$ is negative definite.

The analysis of non-autonomous systems using the theorem above then follows closely the analysis of autonomous systems by means of the invariant set theorem ([SLOTINE; LI, 1991](#); [KHALIL, 2002](#)). Again, we notice that we still have to find a Lyapunov Function to satisfy all the properties cited.

4 Adaptive Control

Models of the airplane dynamics are not exact. There are approximations that may sometimes only work in certain flight regimes, while others depend on parameters that are very hard to measure or calculate precisely. As showed above, however, feedback linearization, and in a less extent, backstepping, depend on the knowledge of the systems dynamics to give disired responses. One way to solve this problem is to use adaptive control schemes ([ASTROM; WITTENMARK, 2008](#); [NAM](#); [ARAPOSTATHIS, 1988](#); [SLOTINE](#); [LI, 1991](#); [SINGH](#); [STEINBERG, 1996](#)).

Nowadays, it can be noted the progressive evolution and application of UAVs (Unmanned Aircraft Vehicles) and MAVs (Micro Aerial Vehicles). The dynamic equations parameters for those types of aircraft are normally not known with the same certainty as for commercial airplanes, also, they are subjected to sudden parameter change (as dropping a load or breaking a fragile command surface). Adaptive controllers then promise to be very useful in those cases.

4.1 Concepts of Adaptive Controllers

The concept of an Adaptive controller is to use the sensor data (both of input as of output) to “check” at each reading of the system, whether the model parameters used are

indeed correct, and if possible, in what direction should they be changed to be coherent with the real data that is being acquired. In the case of nonlinear control, it is very hard to find a general approach to the problem of model adaptation, and the only solutions proposed are based in parameterized models, that is, nonlinear models that are weighted sums of known nonlinear functions:

$$F(X) = \sum_{i=1}^n a_i f_i(X) \quad (4.1)$$

From the aircraft control point of view, that should pose no problems, once the equations of motion can be written in such a way, as seen in chapter 2.

The two simplest concepts of adaptive controllers are the model reference adaptive controller (MRAC) and the self tuning adaptive controller (STC).

4.1.1 The MRAC

A scheme of an MRAC is showed in figure 4.1. Let \hat{a}_i be the vector of estimated parameters. What the MRAC does is to take a desired generic model response to the entry signal and use it as a reference of what the plant was supposed to be doing. As it can be seen, the reference model generates no more then the trajectory one wishes to be following. From the error between the real trajectory and the reference trajectory, the parameters are adapted according to an adequate law an updated in the controller, which will in turn give better inputs to the system that will eventually drive the plant to follow the reference trajectory.

The analysis and design procedure of a MRAC for nonlinear systems has to be done with the use of Lyapunov techniques (NAM; ARAPOSTATHIS, 1988; SINGH; STEIN-

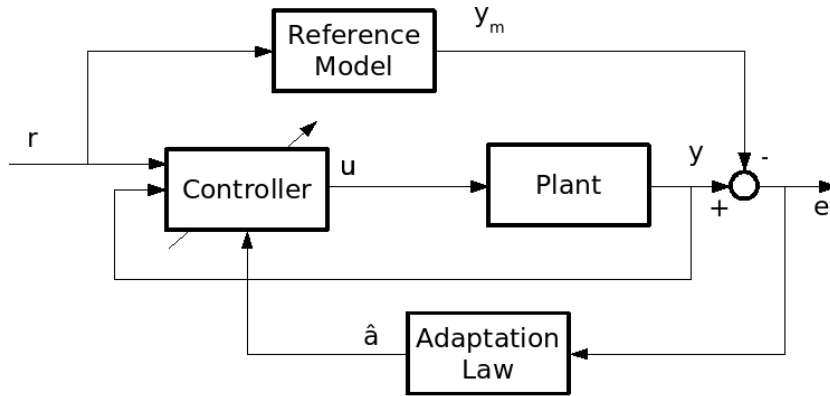


FIGURE 4.1 – The Model Reference Adaptive Controller

BERG, 1996).

Consider first a SISO system. The first step is to create a generalized error function from the error vector. Lets call the generalized error the variable s . This function is normally a linear combination of the error and its derivatives, so that when the error stabilizes at zero the generalized error is also stable at zero and *vice-versa*, for example:

$$s = \sum_{i=1}^{n-1} k_i e^{(i)}$$

where: k_i would be chosen so to that the roots of the polynomial defined by: $\mu(\lambda) = \lambda^n + \sum_{i=0}^{n-1} k_i \lambda^i$ would all have negative real parts.

Then, using the known parameterized dynamics of the model, we write the s dynamics as a function of the real parameters and our control input. As we do not know the value of the real parameters, we are obliged to use a control law dependent of the estimated parameters and the measured state (following the *certainty equivalence principle* (ASTROM;

WITTENMARK, 2008)):

$$u = u(X, \hat{a}_i)$$

A Lyapunov function candidate is proposed for the augmented system in the variables $[s, \hat{a}_i]$ and the control u as well as the adaptation laws $\dot{\hat{a}}_i$ are chosen in such a fashion to render the Lyapunov function candidate time derivative a negative semi-definite function. According to Barballat's lemma, this would guarantee the convergence of the system.

Note that the insertion of the unknown parameters dynamics (over which the designer has complete control) provides an unlimited amount of degrees of freedom, over which one can take advantage to improve the system's dynamic response. On the other hand, overparametrization increases the system complexity and is usually not desired (KRSTIĆ; KANELAKOPOULOS; KOKOTOVIĆ, 1992).

4.1.2 The STC

The *self tuning controller (STC)* as described by figure 4.2 does not rely on a reference model to estimate the plant's parameters. What it does is to take the output and input measurement signals and try to fit the data by adapting the parameters estimates using an estimation algorithm such as the recursive least-squares. These parameters estimates are then passed to the controller (which was previously designed using one of the many possible architectures) and used to calculate the input for the plant to follow a desired trajectory. This process is then recursively repeated in time so that, if the parameters are constant or slowly varying, the total controller scheme will be able to continuously estimate the real plant parameters (in the case of a discrete controller based on time sample analysis, of course this will depend on a high sampling rate).

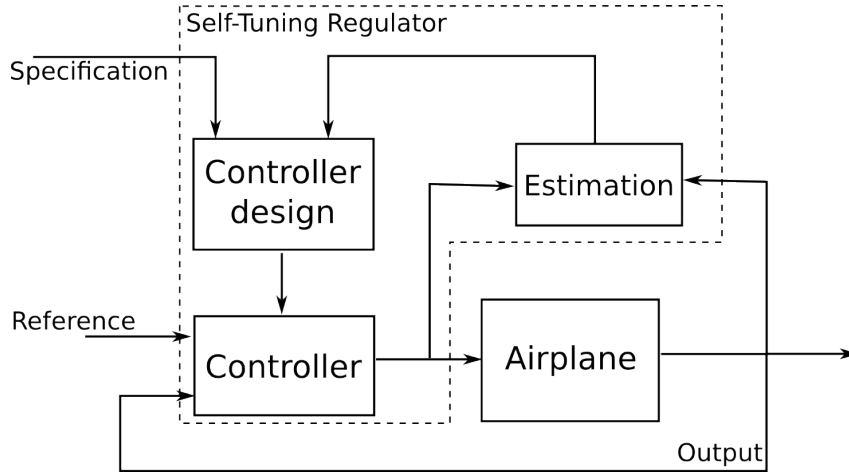


FIGURE 4.2 – The Self Tunning Adaptive Controller. From (ASTROM; WITTENMARK, 2008)

There are many methods available for doing these parameters estimations at each time step and they may or may not contain physical information of the plant that one wishes to control. For linear plants, normally the least-square method or its variations are used (ASTROM; WITTENMARK, 2008; SLOTINE; LI, 1991). These methods can normally be extended to nonlinear plants as well although the stability analysis of a STC controller is more difficult than for the analysis of a MRAC controller. The STC can be extended to stochastic problems. The estimator will be a maximum likelihood estimator in such a case.

One important aspect of the STC controller is that it only “fits” the data received, and this data doesn’t have to be exactly the vectors y and u for example, but filtered and treated versions of it y_f and u_f , so that a linear relation between those last two can be inferred. Finally, easier methods can be used so that parameter convergence and tracking can be guaranteed when using y_f and u_f as inputs for the parameter estimator.

The parameterization of the plant is very important for the self-tuning regulators. One intuitive approach would be to estimate the parameters of the plant (the transfer function in the case of a linear model) and then apply those in the control law as if they

were the true real plant parameter. This is referred to as the *certainty equivalence principle* and the resulting algorithm would be called *indirect adaptive algorithm* (ASTROM; WITTENMARK, 2008). Another approach would be to reparameterize the model such that the controller parameters can be estimated directly. This would be called the *direct adaptive algorithm*.

A close relationship can be traced between the direct adaptive STC approach and the MRAC architecture (refer to (SLOTINE; LI, 1991; ASTROM; WITTENMARK, 2008)). Actually, it can be seen that for some particular controller designs of the STC, the MRAC and the direct STC are equivalent.

4.1.3 Summary of the theory

Adaptive control can be very useful for parameter estimation of nonlinear plants, since the nonlinear controller normally demand a good knowledge of the model to operate adequately. However, the stability analysis of such schemes normally are complex to do, since they augment the complexity of the dynamical system by introducing more parameters.

There are two principal types of adaptive controllers, namely the *model reference adaptive controller* (MRAC) and the *self tuning controller* (STC), which arise from different perspectives (SLOTINE; LI, 1991). In the MRAC scheme the parameters are adapted in such a way to guarantee that the plant will follow a reference dynamical model, while the STC only takes the signal measurements from the input and output of the plant and tries to “fit” this data by constantly updating the estimated parameters. Since this work will only work with the MRAC implementation, the STC was only briefly presented.

5 Adaptive Controller for Load Extraction

5.1 Dynamics of Payload Extraction

As discussed in chapter 2 and detailed in section 2.3, the dynamics of the aircraft is changed by the relative movement of an internal load, as it changes the aircraft's center of gravity.

It is therefore necessary to establish how the load will be extracted, or equivalently what will be the dynamics of the aircraft's center of gravity position during the time the load is being ejected from the fuselage as in figure 5.1.

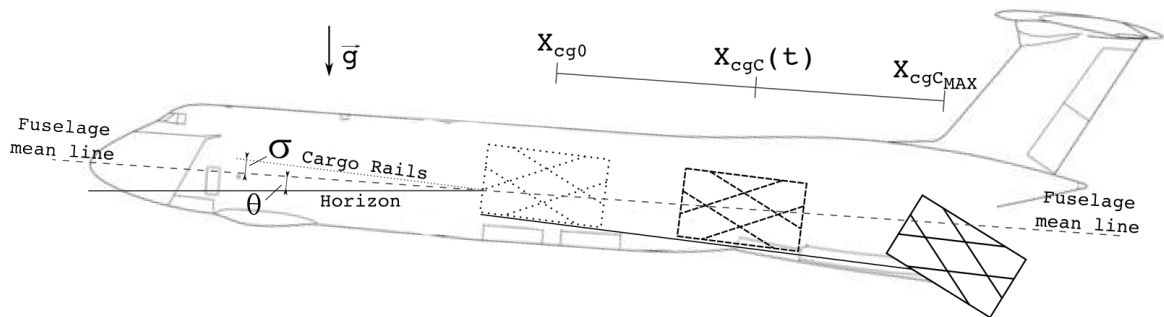


FIGURE 5.1 – Schematics for load positions during extraction

Normally load extraction manouvers are acomplished with the use of parachutes that

use the air resistance to pull the payload out of the airplane. Consider the limit case when there is no parachute and the load is free to slide down the rails only by action of gravity.

As presented in figure 5.1, for this study, the load's center of gravity position (X_{cgC}) is considered to coincide with the empty aircraft center of gravity location (X_{cg0}) just before the ejection command is issued.

Then, the load starts sliding down the rails by action of gravity. Notice that the rails (dotted line in 5.1) have an inclination of σ with respect to the longitudinal axis of the airplane (the dashed line). The dynamics are then described by the classic problem of a mass sliding down an inclined plane with no friction.



FIGURE 5.2 – Interior of a Lockheed Martin's C-5A Galaxy fuselage being loaded. Notice the rails and inclination. (Courtesy of Lockheed Martin).

The airplane chosen for this study was the Lockheed Martin C-5A Galaxy (figure 5.1). A scaled two-sided view of the aircraft and the parameters for its dynamic model are given in appendix A. From the dimensions described in figure A, it is possible to infer the length of the path described by the load inside the aircraft. The relevant parameters

for this case study are presented in table 5.1.

Mass of unloaded aircraft	m_A	248416kg
Mass of the load	m_C	15000kg
Length of the rails	$X_{cgC_{max}} - X_{cg0}$	26.2m
Maximum <i>C.G.</i> displacement	$\Delta X_{cg_{max}}$	1.49m
Initial <i>C.G.</i> position	X_{cg0}	0.30 \bar{c}
<i>C.G.</i> position at extraction	$X_{cg_{max}}$	0.46 \bar{c}
Inclination of cargo ramp	σ	5°

TABLE 5.1 – Parameters of load extraction for the C-5A Galaxy.

Now, back to the dynamic modeling of the sliding load. While inside the aircraft, the load will accelerate according to 5.1:

$$\ddot{X}_{cgC} = g \sin(\sigma + \theta), \quad X_{cgC} < X_{cgC_{max}} \quad (5.1)$$

where σ and θ in equation 5.1 are defined as in figure 5.1. Note that σ is fixed.

Since the equations are being developed as a function of the total CG displacement (ΔX_{cg}) from its original position (X_{cg0}), one can use equations 5.1, 2.21 and 2.22 to find the dynamics for ΔX_{cg} . Substituting 2.22 for X_{cg} in 2.21 one finds:

$$\underbrace{\frac{m_A}{m_A + m_C}}_{\mu_A} (X_{cg0} - X_{cgC}) = \frac{-\mu_A}{(1 - \mu_A)} \Delta X_{cg} \quad (5.2)$$

Taking the second time-derivative of 5.2 and replacing 5.1 for \ddot{X}_{cgC} we have:

$$\Delta \ddot{X}_{cg} = (1 - \mu_a) g \sin(\sigma + \theta), \quad \Delta X_{cgC} < \Delta X_{cgC_{max}} \quad (5.3)$$

During the simulation of the aircraft's flight, equation 5.3 can be used together with initial conditions $\Delta X_{cg}(TE^-) = \Delta X_{cg0}$ and $\Delta \dot{X}_{cg}(TE^-) = 0$ to calculate the current

position of the CG at each time step after the extraction comand instant (TE).

Once the load is extracted ($X_{cgC} = X_{cgC_{max}}$), the simulation must restart from its current state but considering the coefficients, mass and inertia for the unloaded aircraft. This “restart” is accomplished in the software Matlab[®] by the use of the “Events” option of the `ode45` option set (INC., 2000-2012a) in the following manner:

- The simulation starts with the load’s *C.G.* at the same position as the aircraft’s *C.G.*
- At time TE , an extraction command is issued and the load starts sliding down the rails following the dynamics 5.1
- At each integration step, an event function is called to check the load’s *C.G.* position and compare it to its maximum limit $X_{cgC_{max}}$
- When this limit is reached, the integration is stoped. The current time and state are saved and a “load dropped flag” is set to True.
- If the current time is less then the final integration time, which was previously chosen, the integration is then restarted with initial conditions equal to the saved simulation state just before the drop.

5.2 Nonlinear-Adaptive Controller Development

A nonlinear adaptive control law for regulation of the pitch angle using the elevator as the only control input will be developed. It is further assumed the aircraft has the following sensors:

- A rate gyroscope for measuring the pitch angular rate q
- An integrating gyroscope for measuring the pitch angle θ
- Air sensors (pitot, static intake, thermometer) for measuring the dynamic pressure \bar{q} and estimating the aircraft's velocity V
- An accelerometer at the aircraft's center of gravity and aligned with the aeroplane Z body axes.

The derivation of the controller follows Lyapunov's second method as in (SINGH; STEINBERG, 1996; STEINBERG; PAGE, 1998; ASTROM; WITTENMARK, 2008).

Consider the MRAC regulator architecture given by the diagram 5.2.

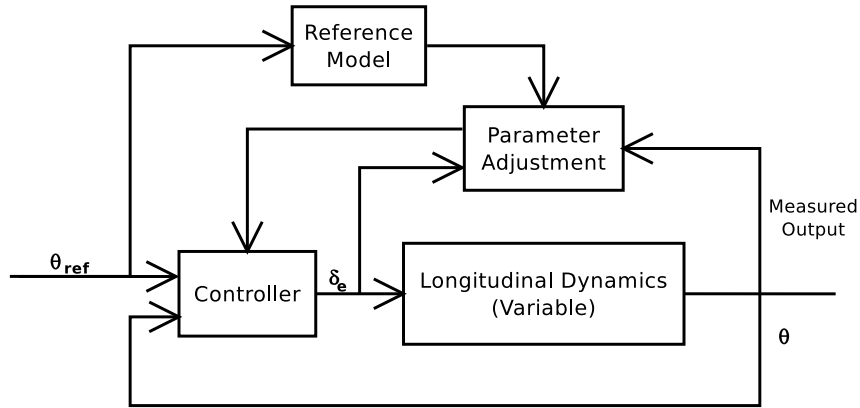


FIGURE 5.3 – Block diagram for a model-reference adaptive controller (MRAC) for pitch control during load extraction.

The objective is to find a control law $d_p(q, \theta, \theta_{ref}, \hat{A}, \hat{b})$ dependent on the estimated parameters and adaptation schemes $\dot{\hat{A}}$ and $\dot{\hat{b}}$ that will stabilize the real aircraft pitch in the reference model's pitch output and at the same time adapt the parameters to their real values.

This can be accomplished by defining a Lyapunov candidate function dependent on the trajectory error and the parameter's estimation errors and defining the control and adaptation laws so that its derivative will be negative semi-definite.

First, though, the *underlying control problem* (as described in (ASTROM; WITTENMARK, 2008)) will be solved using feedback linearization on the fast dynamics. The obtained ideal control will be after compared with the resulting control dependent on the parameter's estimates.

Feedback Linearization Law: Centainty Equivalence From equations 2.17d and 2.17a one finds for the aircrafts fast longitudinal dynamics:

$$\begin{aligned}\dot{\theta} &= q \\ \ddot{\theta} = \dot{q} &= \frac{\mathcal{M} + z_{F/CG} F \cos(\alpha_f) - \dot{I}_{yy} q}{I_{yy}}\end{aligned}\tag{5.4}$$

Expanding the aerodynamic moment in its components the second equation in 5.4 can be written as:

$$\begin{aligned}\ddot{\theta} &= \frac{\bar{q} S \bar{c}}{I_{yy}} \left(C_{\mathcal{M}_0} + C_{\mathcal{M}_\alpha} \alpha + C_{\mathcal{M}_{\dot{\alpha}}} \dot{\alpha} \frac{\bar{c}}{2V_0} + C_{\mathcal{M}_{\dot{q}}} \dot{q} \frac{\bar{c}}{2V_0} + C_{\mathcal{M}_{d_p}} d_p \right) \\ &\quad + \frac{z_{F/CG} F \cos \alpha_f}{I_{yy}} - \frac{\dot{I}_{yy} q}{I_{yy}}\end{aligned}\tag{5.5}$$

Now, as seen in chapter 2, the aerodynamic coefficients in (5.5) will vary with $C.G.$ position. We thus separate the state variables in one vector and the coefficients in another to get:

$$\ddot{\theta} = A_0 + \phi_{A1}^T A_1 + \phi_b^T b \delta_p\tag{5.6}$$

Where:

$$\begin{aligned}
A_0 &= \frac{z_{F/CG} F \cos \alpha_f}{I_{yy}} - \frac{\dot{I}_{yy} q}{I_{yy}} \\
A_1 &= \frac{\bar{q}_0 S \bar{c}}{I_{yy}} \begin{bmatrix} C_{M_0} & C_{M_\alpha} & C_{M_{\dot{\alpha}}} \frac{\bar{c}}{2V_0} & C_{M_{\dot{q}}} \frac{\bar{c}}{2V_0} \end{bmatrix}^T \\
b &= \frac{\bar{q}_0 S \bar{c}}{I_{yy}} C_{M_{d_p}} \\
\phi_{A1} &= \frac{\bar{q}}{\bar{q}_0} [1 \quad \alpha \quad \dot{\alpha} \quad q]^T \\
\phi_b &= \frac{\bar{q}}{\bar{q}_0} \\
\bar{q}_0 &= \frac{1}{2} \rho_0 V_0^2
\end{aligned} \tag{5.7}$$

In equation 5.2 ρ_0 means the air density at sea level and V_0 the airspeed for which the aerodynamic coefficients were estimated.

Let us assume that it is desired to have a dynamics for the pitch angle described by:

$$\ddot{\theta}_m = -k_1 \dot{\theta}_m - k_2 (\theta_m - \theta_{ref}) \tag{5.8}$$

Where k_1 and k_2 make a stable dynamics the the reference model system.

With perfect knowlegde of the system's parameters and a perfect state measurement one finds by dynamic inversion (see chapter 3) that the control:

$$d_p = \frac{1}{\phi_b^T b} \left(-A_0 - \phi_A^T A - k_1 \dot{\theta}_m - k_2 (\theta_m - \theta_{ref}) \right) \tag{5.9}$$

will make the fast dynamics follow the desired model. Since neither the parameters nor the state are known precisely the control law given by 5.9 has to be modified.

Adaptive Feedback Linearization Note first that one can group A_0 and A_1 by augmenting the regression vector ϕ_{A1} to get:

$$\ddot{\theta} = \phi_A^T A + \phi_b^T b d_p \quad (5.10)$$

$$A = [A_0 \quad A_1]^T \quad (5.11)$$

$$\phi_A = [1 \quad \phi_{A1}]^T \quad (5.12)$$

Now consider we only have estimates of the vectors A and b given by \hat{A} and \hat{b} and that the errors in such estimates are given by:

$$\begin{aligned} \tilde{A} &= A - \hat{A} \\ \tilde{b} &= b - \hat{b} \end{aligned} \quad (5.13)$$

Now let us introduce the generalized error s given by:

$$s = \dot{\theta} - \dot{\theta}_m + K(\theta - \theta_m) = q - q_m + K(\theta - \theta_m) \quad (5.14)$$

Following works such as (SINGH; STEINBERG, 1996; ASTROM; WITTENMARK, 2008),

this work proposes the following Lyapunov candidate function V :

$$V = \frac{1}{2}s^2 + \frac{1}{2}\tilde{A}^T P \tilde{A} + \frac{1}{\gamma}\tilde{b}^2$$

we find that:

$$\frac{dV}{dt} = s\dot{s} + \tilde{A}^T P \dot{\tilde{A}} + \frac{2}{\gamma}\tilde{b}\dot{\tilde{b}} \quad (5.15)$$

A hypothesis is need to continue the developement of equation 5.15. From the definition of the parameters errors in equation 5.13 it follows that their time-derivatives will be a sum of the actual parameters time variation with the adapted parameters time variation. The hypothesis assumed is that the true parameters time variation is small enough so that we can consider the following approximation:

$$\begin{aligned}\dot{\tilde{A}} &= -\dot{\hat{A}} \\ \dot{\tilde{b}} &= -\dot{\hat{b}}\end{aligned}\tag{5.16}$$

This is the same as considering that the parameters are “slow varying” with respect to both the aircraft dynamic modes and most importantly the controller adaptation dynamics.

Now, the controller being developed is actually able to track a pitch setpoint, as it will follow any desired model dynamics. For simplicity, let us consider the regulation problem, where $q_m = 0$ and $\theta_m = \theta_{ref}$. In those conditions, derivating equation 5.14 in time gives:

$$\dot{s} = \dot{q} + Kq = \phi_A^T \dot{A} + \phi_b^T \dot{b} d_p + Kq\tag{5.17}$$

Using 5.17, 5.13 and 5.16 in 5.15 one finds:

$$\frac{dV}{dt} = s \left(\phi_A^T \hat{A} + \phi_b \hat{b} d_p + Kq + \phi_A^T \tilde{A} + \phi_b \tilde{b} d_p \right) - \tilde{A}^T P \dot{\hat{A}} - \frac{2}{\gamma} \tilde{b} \dot{\hat{b}}\tag{5.18}$$

Choosing the control law:

$$d_p = \frac{1}{\hat{b}\phi_b} \left(-Kq - \phi_A^T \hat{A} - c_1 s \right)\tag{5.19}$$

Where: $c_1 > 0$

And substituting in equation 5.18 we find that:

$$\frac{dV}{dt} = -c_1 s^2 + s \left(\phi_A^T \tilde{A} + \phi_b \tilde{b} d_p \right) - \tilde{A}^T P \dot{A} - \frac{2}{\gamma} \tilde{b} \dot{b} \quad (5.20)$$

Now we choose the parameter's adaptations to cancel the unknown terms in equation :

$$\dot{A} = s P^{-1} \phi_A \quad (5.21)$$

$$\dot{b} = \frac{\gamma}{2} s \phi_b d_p \quad (5.22)$$

and the derivative of the Lyapunov function becomes:

$$\frac{dV}{dt} = -c_1 s^2 \quad (5.23)$$

This function is negative as long as the measured trajectory is not equal the refence trajectory. In the case of regulating the pitch angle, this will happen as long as the measured pitch angle is not equal to the reference signal or if there is any pitch rate measured by the rate gyro. With the control law in 5.19 and adaptations 5.21 and 5.22 the traking error will thus always go to zero.

Controller implementation Comparing equations 5.9 and 5.19, together with de definition of s in 5.14, it is found that the adaptive control law corresponds to the ideal control law, only by exchanging the real parameter's by the estimated ones.

Notice, however, that according to the definition of ϕ_{A1} in equations 5.2 it would be necessary to measure α and $\dot{\alpha}$ to apply the control law deduced in 5.19. As those measures are not normally available in standard aircraft, they shall be replaced by the considered

measured variables described in the beginning of this section.

Keeping in mind the regulation problem of keeping the pitch for leveled flight, one finds that for such flight conditions:

$$\alpha \approx \theta \quad (5.24)$$

Moreover, considering output from the accelerometer placed in the aircraft's CG and aligned with its vertical axis (see (DUKE; ANTONIEWICZ; KRAMBEER, 1988)), and the expression for $\dot{\alpha}$ as in 2.17c one finds that for small angular rates q it is reasonable to assume:

$$\dot{\alpha} \approx q + \frac{g}{V}(1 - n_z) \quad (5.25)$$

Where n_z is the normalized measure of the accelerometer. Finally, substituting equations 5.24 and 5.25 for the expression of ϕ_A one finds the implementation of the control law and parameter adaptations as:

$$\dot{d}_p = \frac{1}{\hat{b}\phi_b} \left(-Kq - \phi_{Am}^T \hat{A} - c_1 s \right) \quad (5.26)$$

$$\dot{\hat{A}} = sP^{-1}\phi_{Am} \quad (5.27)$$

$$\dot{\hat{b}} = \frac{2}{\gamma} s\phi_b \dot{d}_p \quad (5.28)$$

$$\text{Where: } \phi_{Am} = \begin{bmatrix} 1 & \frac{\bar{q}}{\bar{q}_0} & \frac{\bar{q}}{\bar{q}_0}\theta & \frac{\bar{q}}{\bar{q}_0} \left(q + \frac{g}{V}(1 - n_z) \right) & \frac{\bar{q}}{\bar{q}_0}q \end{bmatrix}$$

K, c_1, P , and γ are parameters chosen by the designer

Equations 5.26 to 5.28, together with definitions and 5.14 form the adaptive control laws for pitch tracking. Which shall be used for pitch regulation with the choice of $q_m = 0$ and $\theta_m = \theta_{ref}$, where θ_{ref} will be the initial trimmed pitch angle in the following simulations.

6 Simulation

6.1 Description

The adaptive controller for load extraction developed in the last chapter was implemented in simulations for the C5A-Galaxy aircraft, described in appendix A. The relevant parameters for the load movement inside the aircraft were described in table 5.1.

The simulations consisted in implementing the dynamic equations for longitudinal flight with varying center of gravity developed in chapter 2 and synthesized in section 2.4. The *C.G.* dynamics was implemented as described in section 5.1. First the trim commands and states were found for a nominal flight condition as described in table 6.1.

Leveled Flight Conditions		Trimmed State and Commands	
H	500 m	$\alpha = \theta$	0.68°
V	75 m/s	d_p	0.06°
ΔX_{cg}	0 m	Throttle	39.8%

TABLE 6.1 – Nominal flight conditions before load extraction

Three cases were studied. One with fixed controls at the trimmed positions for later reference, one with the adaptive controller in action and a last case using a robust H_∞ control approach. Three gain sets were applied on the second case. In the third case, the controller gains were calculate by an expedite automatic process using the structured H_∞ sythesis (GAHINET; APKARIAN, 2011) library of the comercial software Matlab[®]

(INC., 2000-2012b). Simulations were run starting from nominal flight conditions and “activating” the load dynamics at “time of extraction” $TE = 5s$ (for the fixed controls) or $TE = 7s$ (for the controlled cases).

6.2 Results and Discussion

Fixed commands Figure 6.1 shows the simulation results on the states for the load extraction with fixed controls. The red dot in the graphics shows the instant when the load was extracted. The influence of the CG variation is seen clearly by the large fluctuations of angle of attack during and after the load movement.

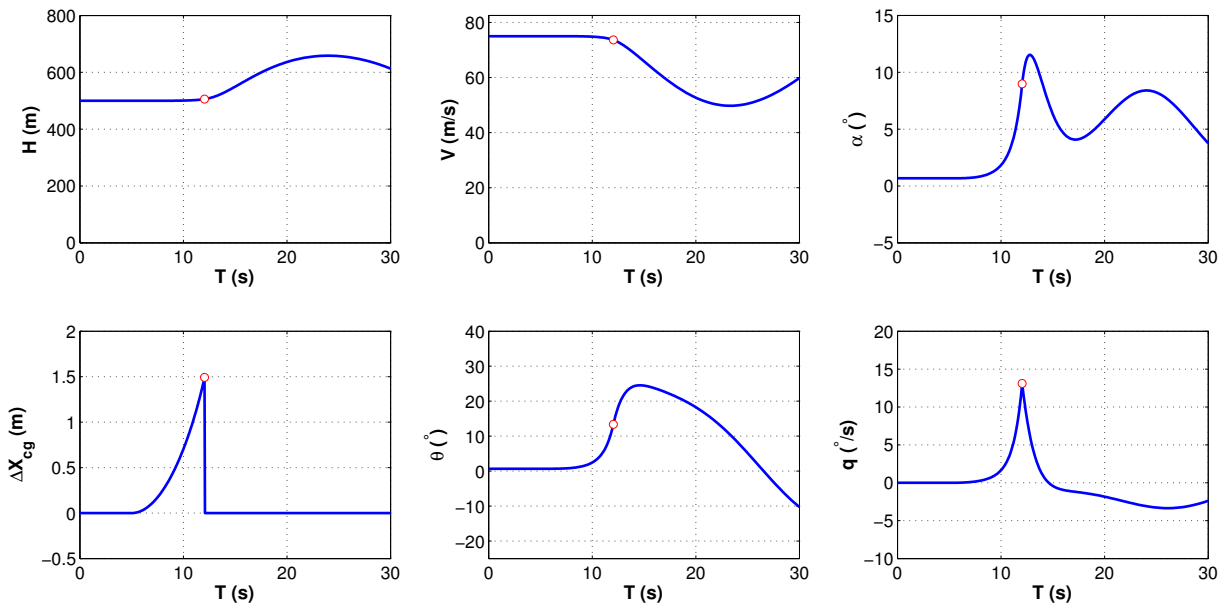


FIGURE 6.1 – Load extraction simulation with fixed commands. Evolution of the states.

The natural, fixed control variation of the parameters which will be adapted is shown in figure 6.2. Notice the sharp change in the parameters values at the moment of extraction.

Also notice that only the fast dynamics parameters (α , θ , and q) change noticeably due to CG movement. The extraction time is was $TE = 12.04s$ meaning it took approximately

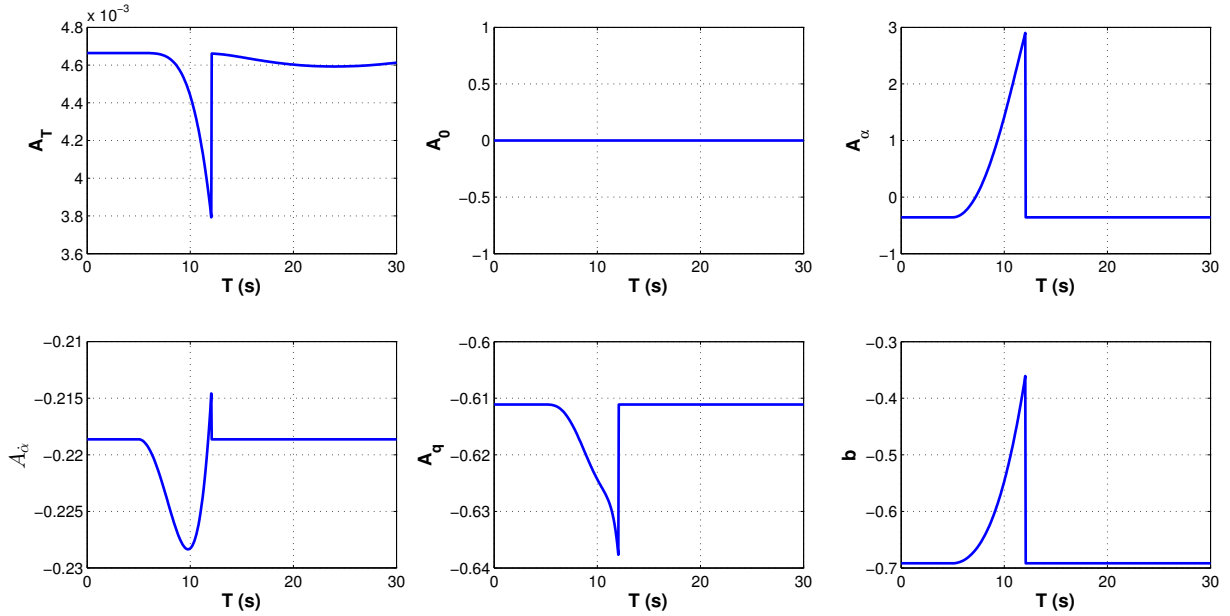


FIGURE 6.2 – Load extraction simulation with fixed commands. Variation of the parameters in parameter vector A_1

7s for the load to travel from the CG to the rear of the aircraft.

Adaptive controller - nominal case Figures 6.3 to 6.5 show the simulation results for the adaptive controller. The controller parameters for this scenario are listed in table 6.2.

K	2
c_1	1
P	$\text{diag}([1 \ 1 \ 1 \ 1 \ 1])$
γ	1

TABLE 6.2 – Controller parameters. Case 1.

It is seen the controller is effective in maintaining the pitch of the aircraft during movement of the load and after that to reestablish the pitch after the load drop.

In figure 6.4 it is noted that the control effort does not impose any saturation problems, although it is certain that a more realistic simulation would impose saturations in the elevator rate.

Yet perhaps the most surprising fact from the adaptation simulation is seen in figure

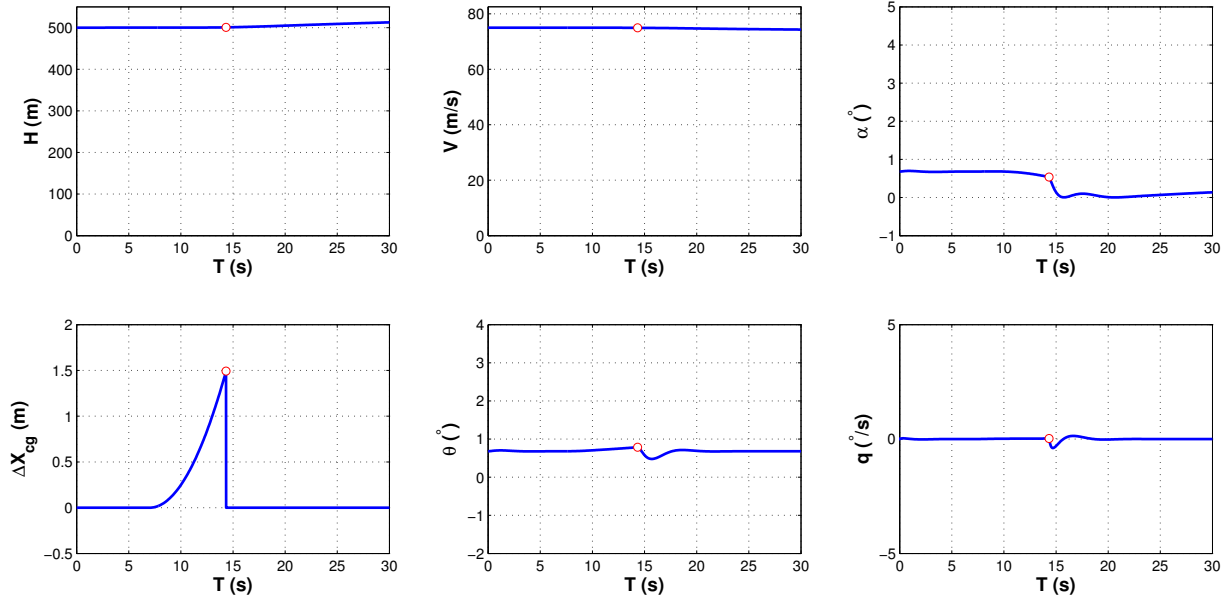


FIGURE 6.3 – Load extraction simulation with the adaptive controller (case 1). Evolution of the states.

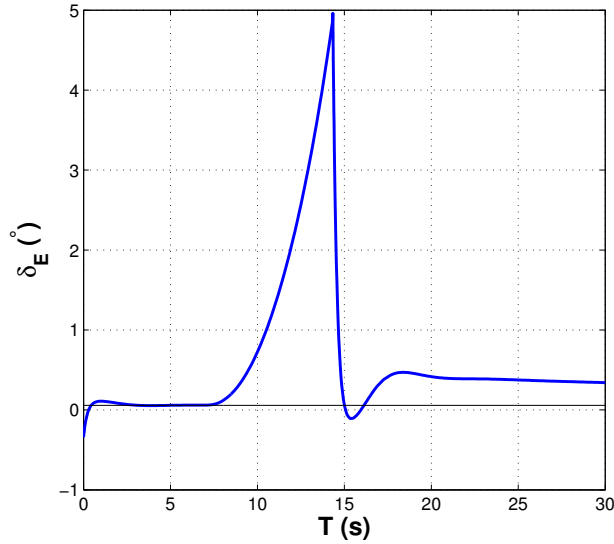


FIGURE 6.4 – Load extraction simulation with the adaptive controller (case 1). Elevator Command.

6.5. The results show a much more effective adaptation of the parameters A_T and A_0 when compared to the adaptations of the other parameters. This suggests that the gains in matrix P should be calibrated if one wants to favour the adaptation of all parameters.

Nevertheless, it can be considered that all the unmodelled dynamics were “absorbed” by the variation of those terms. It is worth studying what would happen if those terms adaptations were shut down and the adaptations of the other terms amplified. This is

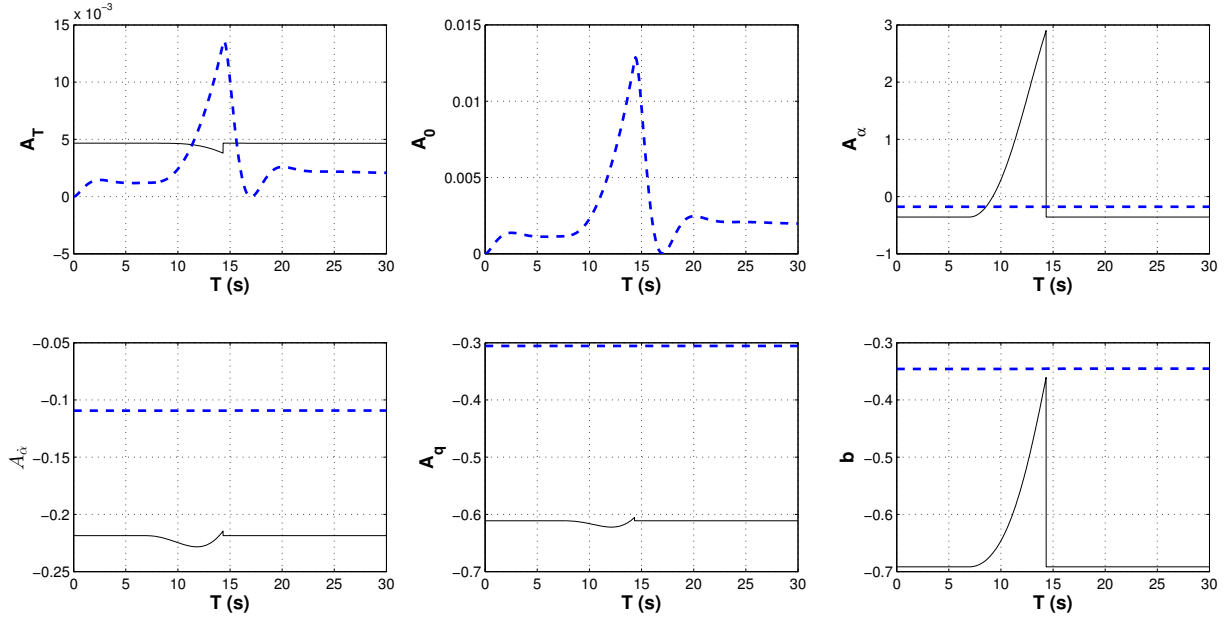


FIGURE 6.5 – Load extraction simulation with the adaptive controller (case 1). Parameter variation and adaptation.

done in case 2.

Adaptive controller - selective adaptation Figures 6.6 to 6.8 show the simulation results for the adaptive controller. The controller parameters for this scenario are listed in table 6.3.

K	2
c_1	1
P	$\text{diag}([0 \ 0 \ 100 \ 100 \ 100])$
γ	100

TABLE 6.3 – Controller parameters. Case 2.

Again the controller was effective in regulating the state without saturation, although it was necessary some more control effort, as shown by figure 6.7.

Comparison with different control strategies In order to further access the performance of our adaptive controller, a robust, structured H_∞ controller was designed for the linearized dynamics of the loaded airplane with the CG in the nominal design position.

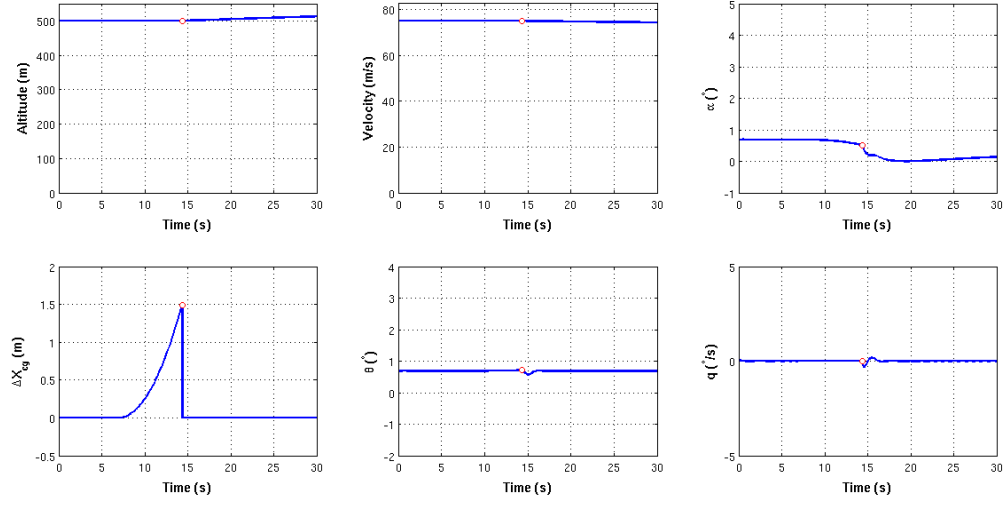


FIGURE 6.6 – Load extraction simulation with the adaptive controller (case 2). Evolution of the states.

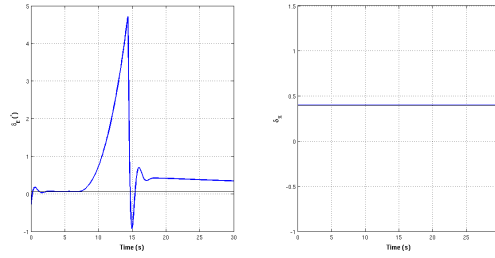


FIGURE 6.7 – Load extraction simulation with the adaptive controller (case 2). Elevator Command.

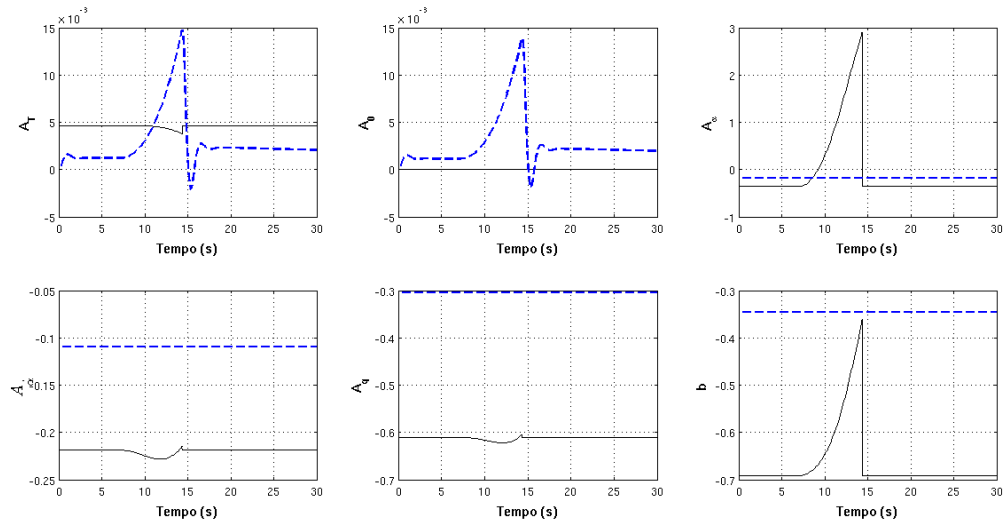


FIGURE 6.8 – Load extraction simulation with the adaptive controller (case 2). Parameter variation and adaptation.

This was done by an expedite design (not optimized) following the procedure outlined in (GAHINET; APKARIAN, 2011) and using the Matlab[®] library recent implementations of the `looptune` function. The reader is referred to the references cited for in depth information of this particular robust controller design and implementation.

This was done in the sole purpose of having a base of comparison for performance of different controllers. Instead of comparing performance between adaptive and classical PI controllers, it was felt more sensible to access a different control strategy that also tries to cope with parameter drift, as is the case of the robust controller here implemented.

For the implementation done in the following simulations, consider the state vector $X = [H \ V \ \alpha \ \theta \ q]^T$ and the command vector $U = [\delta_\pi \ \delta_e]$. The linearized state space model of the system ($\dot{x} = Ax + Bu$) is then given by:

$$A = \begin{bmatrix} 0 & 0 & -75.000 & 75.000 & 0 \\ 0 & -0.029 & 5.367 & -9.807 & 0 \\ 0 & -0.004 & -0.566 & 0.002 & 0.997 \\ 0 & 0 & 0 & 0 & 1.000 \\ 0 & -0.001 & -0.397 & -0.058 & -0.475 \end{bmatrix} \quad B = \begin{bmatrix} 0 \\ 0 \\ -0.037 \\ 0 \\ -0.658 \end{bmatrix}$$

The controller is pitch angle tracker composed of a PI structure with static feedback gain on the pitch rate for damping, given by the block diagram in figure 6.9.

The gains were found using the `looptune` function (GAHINET; APKARIAN, 2011).

The results for the simulation with the robust controller are presented in figures 6.10 and 6.11.

As one sees, the linear controller also gives a proper response, but with a higher level of oscilation and at the expense of little more control effort.

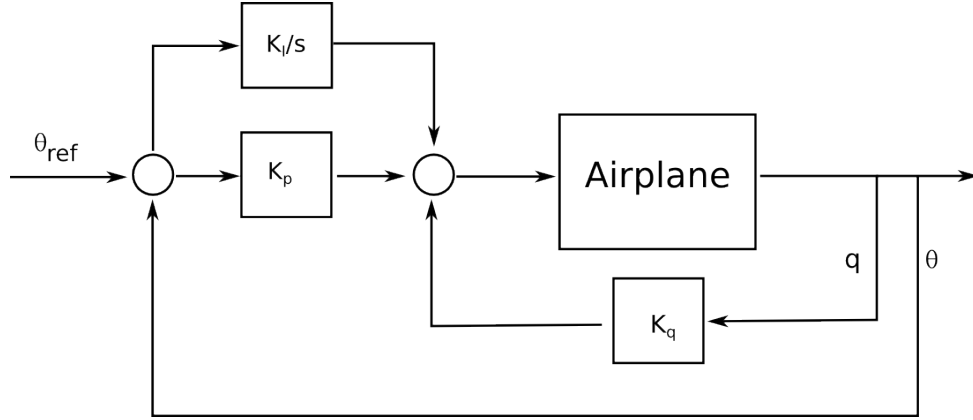
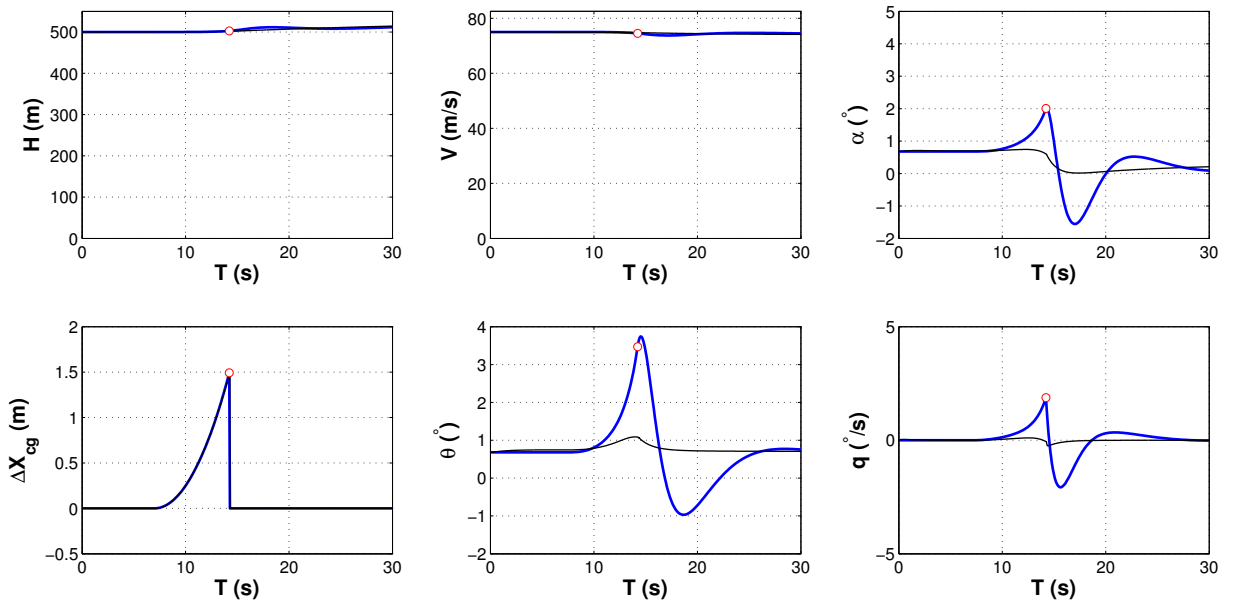
FIGURE 6.9 – Block diagram for the controller to be tuned with structured H_∞ approach.

FIGURE 6.10 – Load extraction simulation with the robust controller. Evolution of the states.

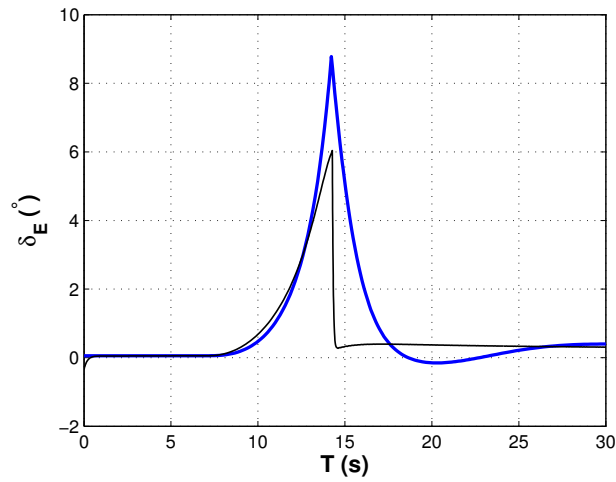


FIGURE 6.11 – Load extraction simulation with the robust controller. Commands.

Following the observations in (ASTROM; WITTENMARK, 2008), the robust controller, by design, will normally have a high inner-loop gain, in order to cope with the plant's variations and still provide a proper response. This will in general produce better responses to “quick” parameter variations (oscillation in parameter occurring in frequencies comparable to the system's dynamic modes) than the adaptive controllers.

On the other hand, for slow varying parameters and large parameter variation, the adaptive controller shows better results. Looking again at equation 5.26 and remembering the definition of s in 5.14 one can write the adaptive controller command as:

$$\delta_p = \underbrace{\frac{-c_1}{\hat{b}\phi_b}(\theta - \theta_m)}_{\text{Proportional}} + \underbrace{\frac{-c_1 - K}{\hat{b}\phi_b}q}_{\text{Derivative}} + \underbrace{\frac{\phi_{Am}^T \hat{A}}{\hat{b}\phi_b}}_{\text{Adaptation}} \quad (6.1)$$

In equation 6.1 we've highlighted the terms as the sum of a proportional term, a derivative term and a final term on the adapting parameters, which, given enough external excitation should converge to the true parameters of the system. Seen this way, the architecture is close to the one chosen for the robust controller, that is, the adaptive controller is a regular controller with continuously changing gains. The term dependent on the system's parameters could be roughly compared to an integrator, in the sense it will change as long as the system is not perfectly following the desired model.

While one can notice there are several interesting aspects to be noted when comparing between the two types of controller simulated, the adaptive and the robust one, this work will not discuss this particular matter. The results from the structured H_∞ controller approach are only presented here as a basis of comparison, so one can take the performance presented for the adaptive controller in a broader context. The reader is referred to (ASTROM; WITTENMARK, 2008; SLOTINE; LI, 1991) for in-depth discussions comparing

several robust/adaptive controller approaches.

7 Final Comments

7.1 Conclusion

This work has shown the feasibility of applying an adaptive controller to the problem of pitch regulation during a payload extraction manouver. The controller design is nonlinear and based on the feedback linearization theory. The adaptive architecture is a Model-Reference Adaptive System (MRAS or MRAC) and the resulting nonlinear-adaptive controller was developed by direct application of Lyapunov's second method.

By comparison with an expedite robust design, structured H_∞ procedure, one can see that the adaptive controller can perform at least as well as the linear robust one, but might offer some advantages. Among the advantages are the operation in more extreme deviations from the nominal flight condition - thanks to the underlying nonlinear controller - and savings on the modelling effort, since a simpler model can be used for the adaptive case, as long as it takes into account all the principal dynamic modes of the system.

There are also drawbacks to be pointed. The complexity of the controller is higher, as given by the augmented state which encompasses the parameter's estimates and the controller parameters such as the model reference and the controller gains. Proofs of stability for the stochastic (real) case are still somewhat limited. Finally, as discussed in

(ASTROM; WITTENMARK, 2008), the robust linear controller can give better responses when fast parameter variation occurs.

The robust linear controller, and other classical linear design techniques must be always considered as an alternative to adaptive control, and the designer must weight the cost and benefits of each approach to a given control problem before choosing a design method over another.

7.2 Suggestions for Future Work

The low cost of high-capacity processing units and sensor electronics has brought the UAV technology well within the range of hobbyists and the academia as a teaching tool. This opens a rich field of activities and experiments for testing innovative control paradigms. Here will be left some suggestions for the continuity of works on the field of nonlinear and adaptive control within the research and teaching community.

Feedback Linearization

- Nonlinear controllers for UAV's can be developed and tested to improve the understanding of aircraft's dynamics and control. A nice challenge is to develop a nonlinear controller capable of doing a closed-loop looping manouver. The use of *quaternions* for the system modelling and control design in such a case would be strongly advised.
- Following the works of controlling aircraft's at a high-angle of attack usign backstepping (HARKEGARD, 2001b), a team could develop controllers for unusual UAV architectures such as tail-sitter airplanes, focusing on the transition of vertical to

normal flight.

- The Zero Dynamics of a typical feedback linearizing pitch angle controller can be further investigated, providing a deeper understanding of the overall stability of such a controller.

Adaptive Control

- The development of a least-square based, self-tuning controller for payload extraction, both in its direct and indirect form, and a comparison of their performances with the MRAC studied in this work.
- Extending the application to the stochastic case, including sensor noise and other random disturbances on the system and using the maximum likelihood adaptive self-tuning controller for a LAPES (Low-Altitude Payload Extraction System).
- Using the adaptive controller architectures to build a “auto-tuner” for simple UAV applications: Suppose an UAV that works on a wide enough flight envelope to request different controller gains to keep the performance parameters under the various flight conditions. An adaptive controller could be used during the development phase in flight tests to find the appropriate system gains, reducing the number of test flights, the control team workload and the overall cost of the flight test campaign.

Payload Extraction Systems

- Test the modifications for the dynamic equations with displacement of the *C.G.* from chapter 2 with the help of more advanced/realistic simulators.
- Implement a feedforward control strategy for payload extraction maneuvers.

Bibliography

- ASTROM, K.; WITTENMARK, B. **Adaptive Control**. New York: Dover, 2008.
- CHEN, J.; SHI, Z. Flight controller design of transport airdrop. **Chinese Journal of Aeronautics**, 2010.
- DUKE, E.; ANTONIEWICZ, R.; KRAMBEER, K. Derivation and definition of a linear aircraft model. **NASA Reference Publication**, 1988.
- ETKIN, B. **Dynamics of Atmospheric Flight**. New York: John Wiley & Sons, 1972.
- FOSSEN, T. I.; STRAND, J. P. **Nonlinear Ship Control (Tutorial Section)**. [S.l.], 1998.
- GAHINET, P.; APKARIAN, P. Structured h_∞ synthesis in matlab. **Preceedings IFAC 2011**, 2011.
- HARKEGARD, O. **Backstepping Designs for Aircraft Control: What is there to gain?** [S.l.], 2001.
- HARKEGARD, O. **Flight Control Design Using Backstepping**. Dissertação (Mestrado) — Linkopings Universitet, 2001.
- HARMANN, G.; HARVEY, C.; STEIN, G.; CARLSON, D.; HENDRICK, R. **F-8C Adaptive Flight Control Laws**. [S.l.], 1977.
- HEFFLEY, R.; WAYNE, F. **Aircraft Handling Qualities Data**. [S.l.], 1972.
- INC., T. M. **MATLAB**. 2000–2012. <http://www.mathworks.com/help/matlab/ref/odeset.html>.
- INC., T. M. **MATLAB**. 2000–2012. <http://www.mathworks.com/products/matlab/>.
- ISIDORI, A. **Nonlinear Control Systems**. 3rd. ed. New Jersey: Springer-Verlag, 1995.
- KHALIL, H. K. **Nonlinear Systems**. 3rd. ed. New Jersey: Prentice-Hall, 2002.
- KRSTIĆ, M.; KANELAKOPOULOS, I.; KOKOTOVIĆ, P. V. Adaptive nonlinear control without overparametrization. **Systems & Control Letters**, v. 19, p. 177–185, 1992.
- MONAHEMI, M. M.; KRISTIĆ, M. Control of wing rock motion using adaptive feedback linearization. **Journal of Guidance, Control, and Dynamics**, v. 19, n. 4, p. 905–912, 1996.

- NAM, K.; ARAPOSTATHIS, A. A model reference adaptive control scheme for pure-feedback nonlinear systems. **IEEE Transactions on Automatic Control**, v. 33, n. 9, p. 803–811, 1988.
- NELSON, R.; SMITH, S. **Flight Stability and Automatic Control**. New York: McGraw-Hill, 1989.
- ROBINSON, A. C. **On the Use of Quaternions in Simulation of Rigid-Body Motion**. [S.l.], 1958.
- ROSKAM, J. **Airplane Flight Dynamics and Automatic Flight Controls - Part I**. Lawrence, KS: Design, Analysis and Research Corporation (DARcorporation), 2001.
- RUTAN, E. L.; STROUP, F. B. **Evaluation of the C-130E Sability and Control Characteristics During Tandem, Sequential, and Single-Paltform LAPES Delivery and Airdrop Deliveries**. [S.l.], 1967.
- SCHLICHTING, H.; TRUCKENBRODT, E. **Aerodynamics of the Airplane**. New York: McGraw-Hill, 1979.
- SHAOXIU, O.; CHONGSHUN, D. The study on the dynamic characteristics of aircraft with cargos moving in its cargo cabin. **Flight Dynamics**, 2011.
- SINGH, S.; STEINBERG, M. Adaptive control of feedback linearizable nonlinear systems with application to flight control. **Journal of Guidance, Control, and Dynamics**, v. 19, n. 4, p. 871–877, 1996.
- SLOTINE, J.-J. E.; LI, W. **Applied Nonlinear Control**. Englewood Cliffs, New Jersey: Prentice-Hall, 1991.
- STEIN, G. Adaptive flight control: A pragmatic view. In: NARENDRA, K.; MONOPOLI, R. (Ed.). **Applications of Adaptive Control**. New York: Academic Press, 1980.
- STEINBERG, M. L.; PAGE, A. **Nonlinear Flight Control with a Backstepping Design Aproach**. [S.l.], 1998.
- STEVENS, B. L.; LEWIS, F. L. **Aircraft Control and Simulation**. [S.l.]: Wiley-IEEE, 2003.
- TENENBAUM, R. A. **Fundamentals of Applied Dynamics**. 175 Fifth Avenue, New York: Springer-Verlag, 2003.
- YANLI, F.; ZHONGKE, S.; WEI, T. **Dynamics modeling and control of large transport aircraft in heavy cargo extraction**. [S.l.], 2011.
- YIMENG, T.; WEIGUO, Z.; BAONING, L. Design of longitudinal control system during airdrop based on adaptive dynamic inversion theory. **Computer Measurement and Control**, 2011.

Appendix A - Aircraft Model

The aircraft's parameters used in this work belongs to the Lockheed Martin's C-5A Galaxy in "Power Approach Configuration" as presented in (HEFFLEY; WAYNE, 1972).

Dimensions presented are in *inches*.

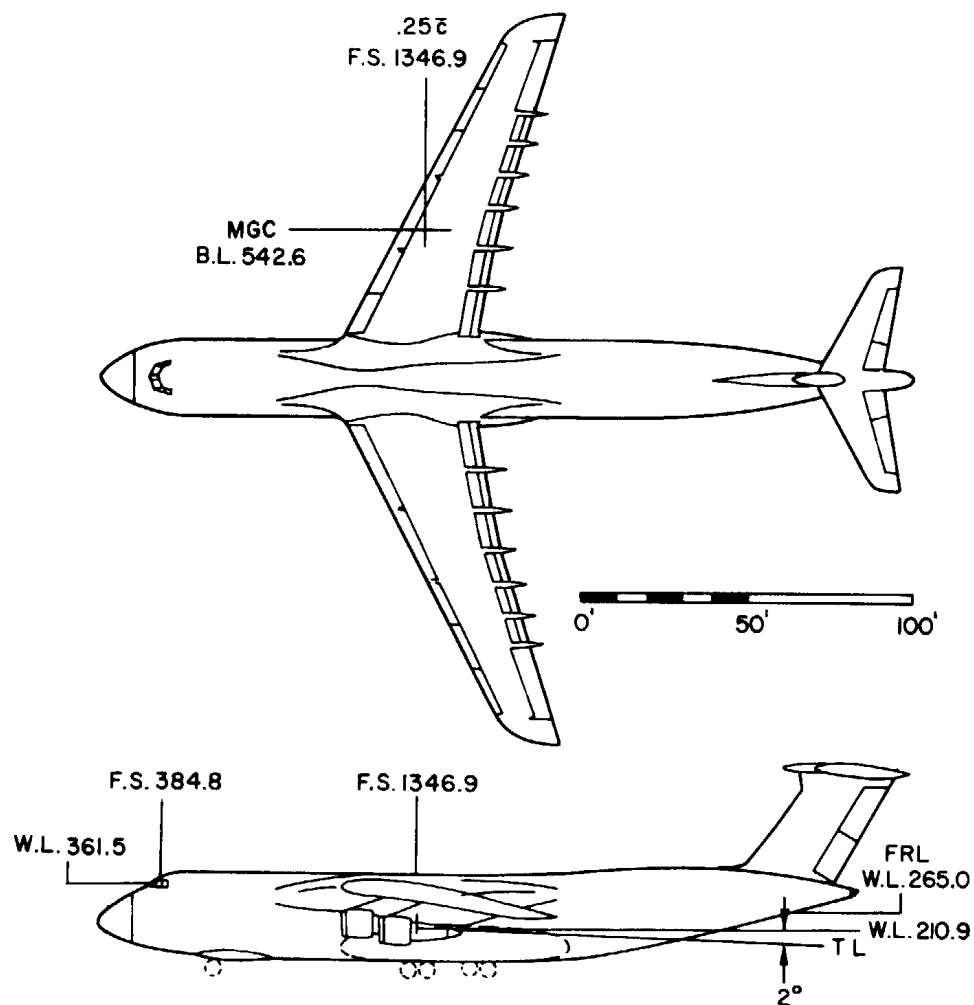


FIGURE A.1 – Top and side view of the C-5A. ((HEFFLEY; WAYNE, 1972))

Galaxy C-5A

Dimensions:	
$S_{ref} = 6200 ft^2$	$\bar{c} = 30.1 ft$
Weight and Inertia:	
$W = 580723 lb$	$I_{yy} = 31.3 \times 10^6 slug - ft^2$
Propulsion:	
$F_{max} = 4 \times 190000 N$	(4x GE TF-39-1C)
$\alpha_f = 2^\circ$	$V_0 = 247 fps$
$n_\rho = 1$	$n_V = 0$
Aerodynamics:	
$C_{L0} = 1.29$	$C_{M0} = 0$
$C_{L\alpha} = 6.08$	$C_{M\alpha} = -0.827$
$C_{L\dot{\alpha}} = -1.14$	$C_{M\dot{\alpha}} = -8.3$
$C_{Lq} = 0$	$C_{Mq} = -23.2$
$C_{L\delta_p} = 0.385$	$C_{M\delta_p} = -1.6$
$C_{D0} = 0.145$	$C_{D\alpha} = 0.622$

TABLE A.1 – C-5A at Power Approach Configuration. Mass, dimensions and longitudinal parameters.

FOLHA DE REGISTRO DO DOCUMENTO

1. CLASSIFICAÇÃO/TIPO <div style="text-align: center;">DM</div>	2. DATA 30 de janeiro de 2013	3. REGISTRO Nº DCTA/ITA/DM-113/2012	4. Nº DE PÁGINAS 88
5. TÍTULO E SUBTÍTULO: Nonlinear adaptive control system for payload extraction operations			
6. AUTOR(ES): Gustavo Oliveira Violato			
7. INSTITUIÇÃO(ÕES)/ÓRGÃO(S) INTERNO(S)/DIVISÃO(ÕES): Instituto Tecnológico de Aeronáutica - ITA			
8. PALAVRAS-CHAVE SUGERIDAS PELO AUTOR: Controle de aeronaves; Sistemas não-lineares; Controle adaptativo; Alijamento de carga; Simulações computacionais; Engenharia aeronáutica			
9. PALAVRAS-CHAVE RESULTANTES DE INDEXAÇÃO: Controle de aeronaves; Sistemas não-lineares; Controle adaptativo; Alijamento de cargas; Simulação computadorizada; Engenharia mecânica; Engenharia aeronáutica.			
10. APRESENTAÇÃO: <div style="text-align: right;"> <input checked="" type="checkbox"/> Nacional <input type="checkbox"/> Internacional </div> ITA, São José dos Campos. Curso de Mestrado. Programa de Pós-Graduação em Engenharia Aeronáutica e Mecânica. Área de Mecânica do Voo. Orientador: Pedro Paglione. Defesa em 14/12/2012. Publicada em 2012.			
11. RESUMO: <p>This work covers the development of a nonlinear, adaptive control system for payload extraction operations. Load extractions are a critical type of maneuver which could make the longitudinal flight dynamics unstable. The online adaptation control strategy seems adequate for the problem, since it can deal with the drift in the plant parameters caused by the movement of the load inside the aircraft. The effects of a continuously varying C.G. position on the longitudinal flight dynamics are modeled in detail. The controller proposed consists on applying the technique of nonlinear inversion coupled with a model reference adaptive controller to deal with the unmodeled/unknown dynamics. The dynamic system considered for the control problem consists of the modeled aircraft dynamics augmented by the unknown parameters - whose dynamics are controlled by the chosen adaptation laws. The demonstration of stability for the complete system is done via Lyapunov's stability theorem for nonlinear dynamic systems. A suitable Lyapunov Function Candidate used for such a demonstration is proposed in this work. Simulation results are presented and discussed based on the theory and on comparison with other control methods performance when applied to the same problem.</p>			
12. GRAU DE SIGILO: <div style="display: flex; justify-content: space-between;"> (X) OSTENSIVO () RESERVADO () CONFIDENCIAL () SECRETO </div>			